

# Mass spectrum of 2-dimensional $\mathcal{N} = (2, 2)$ super Yang-Mills theory on the lattice

---

D. August,<sup>a</sup> B. H. Wellegehausen,<sup>a</sup> A. Wipf<sup>a</sup>

<sup>a</sup>*Friedrich-Schiller University Jena, Theoretisch-Physikalisches Institut, Germany*

*E-mail:* [daniel.august@uni-jena.de](mailto:daniel.august@uni-jena.de), [bjoern.wellegehausen@uni-jena.de](mailto:bjoern.wellegehausen@uni-jena.de),  
[wipf@tpi.uni-jena.de](mailto:wipf@tpi.uni-jena.de)

**ABSTRACT:** In the present work we analyse  $\mathcal{N} = (2, 2)$  supersymmetric Yang-Mills (SYM) theory in two dimensions by means of lattice simulations. The theory arises as dimensional reduction of  $\mathcal{N} = 1$  SYM theory in four dimensions. As in other gauge theories with extended supersymmetry, the classical scalar potential has flat directions which may destabilize numerical simulations. In addition, the fermion determinant need not be positive and this sign-problem may cause further problems in a stochastic treatment. We demonstrate that  $\mathcal{N} = (2, 2)$  super Yang-Mills theory has actually no sign problem and that the flat directions are lifted and thus stabilized by quantum corrections. Only the bare mass of the scalars experience a finite additive renormalization in this finite theory. On various lattices with different lattice constants we determine the scalar masses and hopping parameters for which the supersymmetry violating terms are minimal. By studying four Ward identities and by monitoring the  $\pi$ -mass we show that supersymmetry is indeed restored in the continuum limit. In the second part we calculate the masses of the low-lying bound states. We find that in the infinite-volume and supersymmetric continuum limit the Veneziano-Yankielowicz super-multiplet becomes massless and the Farrar-Gabadadze-Schwetz super-multiplet decouples from the theory. In addition, we estimate the masses of the excited mesons in the Veneziano-Yankielowicz multiplet. We observe that the gluino-glueballs have comparable masses to the excited mesons.

---

## Contents

<b>1</b>	<b>Introduction</b>	<b>1</b>
<b>2</b>	<b><math>\mathcal{N} = (2, 2)</math> SYM theory in two dimensions</b>	<b>4</b>
2.1	Expected mass spectrum	7
2.2	Supersymmetry restoration in the continuum limit	8
2.3	Euclidean formulation	9
2.4	Ward identities	10
<b>3</b>	<b>Lattice formulation</b>	<b>10</b>
3.1	Sign problem and flat directions	11
3.2	Scalar and fermion mass fine tuning	12
3.3	Scale setting and lattice spacing	14
3.4	Smearing	15
<b>4</b>	<b>Restoration of Ward identities</b>	<b>16</b>
4.1	Extrapolation to the chiral limit	17
<b>5</b>	<b>Mass spectrum</b>	<b>20</b>
5.1	Volume dependence	21
5.2	Mesons	21
5.3	Gluino-glueball	24
5.4	Glue- and scalarballs	25
<b>6</b>	<b>Conclusions</b>	<b>26</b>
<b>A</b>	<b>Exact lattice Ward identities</b>	<b>28</b>

---

## 1 Introduction

Many extensions of the standard model of particle physics make use of supersymmetry in order to cure well-known flaws of the standard model, as for instance the hierarchy problem. Some of the additional particles of supersymmetric (susy) gauge theories may be identified as dark matter particles in the universe. Since no additional particles have been observed in experiments up to now it is of utmost interest to investigate the spectrum of susy gauge theories, in particular in the strongly coupled regime. The most simple supersymmetric gauge theories are probably the  $\mathcal{N} = 1$  Super-Yang-Mills (SYM) theories with gauge groups  $SU(N)$ . These are supersymmetric extensions of  $SU(N)$  Yang-Mills theories [1, 2]. For  $SU(3)$  the bosonic sector is identical to that of QCD. It describes the gluons of strong interaction in interaction with their superpartners, the gluinos. The gluinos

are Majorana fermions transforming in the adjoint representation of the gauge group. Like in QCD, the theory is asymptotically free and it is expected, that the gluons and gluinos are confined in colorless bound states. But differently from one-flavor QCD, the  $U(1)_A$  chiral symmetry is anomalously broken only to the discrete subgroup  $\mathbb{Z}_{2N}$ . At low temperatures this symmetry is further broken spontaneously to  $\mathbb{Z}_2$  by the formation of a gluino condensate and thus gives rise to  $N$  physically equivalent vacua [3].

The SYM-theory has a richer spectrum of colour-blind bound states as QCD since the gluinos are in the adjoint representation. Beside (adjoint) mesons, baryons and glueballs, hybrid bound states of gluons and gluinos are expected to show up in the low energy spectrum. Implementing symmetries and anomalies of the theory, low energy effective actions have been proposed [4–6] describing the supersymmetric spectrum of bound states. Thereby the chiral multiplet containing the adjoint  $f$  and  $\eta$  meson is extended to a supermultiplet by a gluino-glueball. A second multiplet contains a  $0^+$  glueball, a  $0^-$  glueball and in addition a gluino-glueball. The low-energy effective action depends on free parameters and hence it is not clear which multiplet is the lighter one. Various arguments were given for both scenarios, see [4–7]. Another difficulty stems from the fact, that for every state in the first multiplet there exists a state in the second multiplet with the same quantum numbers. This mixing of states may lead to an even more complex multiplet structure.

Similarly as QCD the  $\mathcal{N} = 1$  SYM-theory is strongly coupled at low energies and non-perturbative methods are necessary to investigate its mass spectrum. We simulate the theory on a discrete spacetime lattice. This is a non-trivial task since a lattice regularisation breaks supersymmetry explicitly. This can be seen from the susy algebra

$$\{\mathcal{Q}, \mathcal{Q}\} \propto P_\mu,$$

where  $\mathcal{Q}$  is a generator of supersymmetry and the  $P_\mu$  generate translations in space and time. Since a discrete lattice does not admit arbitrary small translations, we can not preserve the full supersymmetry on a lattice, similar to chiral symmetry. In order to recover both symmetries in the continuum limit, certain parameters have to be fine-tuned, making simulations more expensive. Fortunately for  $\mathcal{N} = 1$  SYM theory, the only relevant operator that breaks supersymmetry (softly) is a non-vanishing gluino condensate which at the same time breaks chiral symmetry. Thus it suffices to restore chiral symmetry in the continuum limit to recover supersymmetry [8], making chiral Ginsparg-Wilson fermions the preferred choice [9–11]. Unfortunately chiral fermions are computationally very expensive such that it seems to be more efficient to fine-tune the bare gluino mass parameter of Wilson fermions. For the gauge group  $SU(2)$  with Wilson fermions, the theory has been extensively investigated by the DESY-Münster collaboration [12–19]. Their results confirm the formation of the predicted super-multiplets and reveal, that the glueballs are heavier than the mesons. Simulations for the gauge group  $SU(3)$  are underway [20, 21].

Another strategy is to look at the dimensionally reduced model, namely  $\mathcal{N} = (2, 2)$  SYM-theory in two dimensions. By calculating the mass spectrum of this related and simpler model we should get further insights into the four-dimensional model. The two-dimensional super-renormalizable descendant of the four-dimensional theory allows for larger lattices and

much better statistics. This will lead to a mass spectrum with less statistical errors as in four dimensions.

A first numerical simulation of the two-dimensional model was presented in [22, 23], where the dimensional reduction was done for the lattice theory with compact link variables. Accordingly the scalar fields in the reduced model appear in the exponent of the compact link variables. In the simulation the quenched configurations were reweighted with the Pfaffian. Because of large (statistical) errors the results for Ward identities were inconclusive.

Apart from being a descendant of SYM-theory in four dimensions, the  $\mathcal{N} = (2, 2)$  theory in two dimensions has further interesting properties. Theoretical arguments [24, 25] and numerical calculations based on a discretized light cone quantization [26, 27], both suggest massless states in the physical spectrum. This massless super-multiplet is not seen in four dimensions. Furthermore, it has been conjectured that dynamical susy breaking may occur in the theory [28]. Recent lattice results for the vacuum energy however show no sign of susy breaking [29].

The  $\mathcal{N} = (2, 2)$  theory is the simplest gauge theory which admits a conserved and nilpotent supercharge. This is possible because there are four supercharges from which one can build *one* nilpotent supercharge  $\mathcal{Q}$ . On a lattice only the subalgebra generated by nilpotent supercharges can be realized. Several  $\mathcal{Q}$ -exact lattice models were proposed [30–32]. All these models suffer from the following problem: Usually one can expand the link variables as  $U_\mu = \mathbb{1} + iaA_\mu + \dots$ , in which case we expect an unique vacuum state. This is not the case in all three models proposed and thus one expects an ambiguous continuum limit. In the models in [30, 31] the problem is solved by adding the susy-breaking term  $\mu^2 \text{tr} (U^\dagger U - \mathbb{1})^2$  to the Lagrangian, which dynamically picks a unique vacuum state. In the limit  $\mu \rightarrow 0$ , supersymmetry is then recovered in this construction. In contrast, by deforming the model [32] the unphysical vacuum states can be removed without breaking the nilpotent supersymmetry explicitly [33]. Several numerical investigations show the restoration of the full susy (not only the nilpotent one) [34–40]. The relations between these models were investigated in [41–44]. For a more detailed overview see the reviews [45–49].

Two-dimensional continuum gauge theories have less dynamical degrees of freedom as four-dimensional ones and thus we may expect that topology of the (Euclidean) spacetime becomes more important. In our work we use periodic lattices which discretize a two-torus. In the works [50–52] different lattices with other spacetimes were scrutinized. In particular a generalized topological twisting on generic Riemann surfaces in two dimensions [50] have been considered. The authors revealed the connection of the sign problem, which is absent on the torus, to the  $U(1)_A$  anomaly. With a so called compensator the sign problem can be solved on Riemann surfaces with genus  $\neq 1$ . Ward identities and the  $U(1)_A$  anomaly – the latter is intimately related to the zero modes of the Dirac operator – have been looked at.

The paper is organized as follows: In section 2 we introduce the  $\mathcal{N} = (2, 2)$  theory, discuss its continuum properties and in particular the expected particle spectrum. There is only one relevant operator  $\text{tr} \phi^2$  that needs to be fine-tuned to recover susy in the continuum limit. The corresponding mass-parameter is calculated to one-loop order. To investigate the restoration of susy we derive three independent Ward identities. In section 3 we introduce

our lattice formulation with Wilson fermions and discuss some technical points like the fermion sign problem, potentially flat directions of the effective potential and fine-tuning of the bare parameters. Since susy is broken at finite lattice spacing, the Ward identities are not fulfilled. The additional contributions at finite lattice spacing are discussed in section 4 together with our simulation results concerning the restoration of supersymmetry in the continuum and thermodynamic limit. We shall see that the model has no sign problems in the simulations. The flat directions are lifted and we see no instabilities in the scalar subsector. In section 5 we present our accurate results for the masses of the low lying bound states. One super-multiplet becomes massless in the thermodynamic and supersymmetric limit and a second super-multiplet decouples from the theory. In addition we see a massive super-multiplet of excited states. At the end we present our conclusions in section 6.

## 2 $\mathcal{N} = (2, 2)$ SYM theory in two dimensions

In this section we will derive  $\mathcal{N} = (2, 2)$  supersymmetric Yang-Mills (SYM) theory in two dimensions by a dimensional torus-reduction from  $\mathcal{N} = 1$  SYM theory in four dimensions. We begin with reviewing some relevant properties of the four-dimensional theory [1, 2]. The action is given by

$$S = \int d^4x \operatorname{tr} \left( -\frac{1}{4} F_{MN} F^{MN} + \frac{i}{2} \bar{\lambda} \Gamma^M D_M \lambda \right), \quad (2.1)$$

where capital indices  $M, N$  assume the values 0, 1, 2, 3, the matrices  $\Gamma^M$  build an irreducible representation of the four-dimensional Clifford algebra and  $F_{MN}$  is the field strength tensor

$$F_{MN} = \partial_M A_N - \partial_N A_M - ig [A_M, A_N] \quad (2.2)$$

with gauge potential  $A_M$  in the adjoint representation of the gauge group  $SU(N)$ . The gauge potential and Majorana-field are components of the same super-field such that  $\lambda$  transforms under the adjoint representation as well. Hence, the covariant derivative of the Majorana fermion is

$$D_M \lambda = \partial_M \lambda - ig [A_M, \lambda]. \quad (2.3)$$

The action (2.1) is invariant under the on-shell supersymmetry transformations

$$\delta_\varepsilon A_\mu = i\bar{\varepsilon} \Gamma_\mu \lambda, \quad \delta_\varepsilon \lambda = iF^{MN} \Sigma_{MN} \varepsilon, \quad \delta_\varepsilon \bar{\lambda} = -i\bar{\varepsilon} F^{MN} \Sigma_{MN} \quad (2.4)$$

with  $[\Gamma_M, \Gamma_N] = 4i \Sigma_{MN}$ . These transformations are generated by  $\bar{\varepsilon} Q$ , where  $\varepsilon$  is a constant anticommuting Majorana-valued parameter and the  $\{Q^\alpha\}$  are the four components of the Majorana-valued supercharge  $Q$ . The Majorana condition relates the four entries of a spinor according to  $\lambda = \lambda_c = \mathcal{C} \bar{\lambda}^\top$ , where  $\mathcal{C}$  is a charge conjugation matrix.

The action is also invariant under global  $U(1)_A$  transformations

$$\lambda \rightarrow e^{i\alpha \Gamma_5} \lambda \quad \Gamma_5 = i\Gamma^0 \Gamma^1 \Gamma^2 \Gamma^3. \quad (2.5)$$

In the quantum theory, this chiral symmetry is broken down to  $\mathbb{Z}_{2N}$  via instantons. If a chiral condensate  $\langle \bar{\lambda}\lambda \rangle \neq 0$  forms, it is further broken spontaneously to  $\mathbb{Z}_2$

$$U(1)_A \xrightarrow{\text{instantons}} \mathbb{Z}_{2N} \xrightarrow{\langle \bar{\lambda}\lambda \rangle} \mathbb{Z}_2. \quad (2.6)$$

The  $2N$  physically equivalent vacua are related by the discrete chiral rotations

$$\lambda \rightarrow \exp\left(i\frac{n\pi}{N}\Gamma_5\right)\lambda, \quad n = 0, 1, 2, \dots, N-1. \quad (2.7)$$

Lattice simulations of four-dimensional  $\mathcal{N} = 1$  SYM show that chiral symmetry is indeed spontaneously broken at zero temperature and restored above a critical temperature [17].

The two-dimensional  $\mathcal{N} = (2, 2)$  SYM theory can be derived from the four-dimensional theory via a Kaluza-Klein torus reduction. Thereby one compactifies two directions on a torus such that  $\mathbb{R}^4 \rightarrow \mathbb{R}^2 \times \mathcal{T}^2$  and assumes, that the fields are constant on the torus, e.g.  $\partial_M \lambda = 0$  for  $M = 2, 3$ . The remaining non-compact coordinates are  $x^\mu$  with  $\mu \in \{0, 1\}$ . Although the reduction does not depend on the particular representation of the four-dimensional  $\Gamma$  matrices, it is convenient to choose a particular one:

$$\Gamma_\mu = \mathbb{1} \otimes \gamma_\mu, \quad \Gamma_2 = i\sigma_1 \otimes \gamma_5, \quad \Gamma_3 = i\sigma_3 \otimes \gamma_5, \quad \Gamma_5 = \sigma_2 \otimes \gamma_5 \quad (2.8)$$

with  $\gamma_5 = \gamma_0\gamma_1$ . In this representation, the charge conjugation matrices in two and four dimensions are related as  $C_4 = \mathbb{1} \otimes C_2$  and satisfy

$$C_2\gamma_\mu C_2^{-1} = -\gamma_\mu^T \quad \Longrightarrow \quad C_4\Gamma_M C_4^{-1} = -\Gamma_M^T. \quad (2.9)$$

In a Majorana representation with purely real or imaginary  $\gamma_\mu$  we may choose  $C_2 = -\gamma^0$ . Applying the dimensional reduction to the Yang-Mills Lagrangian yields

$$-\frac{1}{4}F_{MN}F^{MN} = -\frac{1}{4}F_{\mu\nu}F^{\mu\nu} + \frac{1}{2}D_\mu\phi_m D^\mu\phi_m + \frac{g^2}{4}[\phi_m, \phi_n][\phi^m, \phi^n], \quad (2.10)$$

where the first term on the right hand side is the two-dimensional Yang-Mills Lagrangian, the second term a kinetic term for the two adjoint scalar fields  $\phi_m = A_{m+1}$  with  $m \in \{1, 2\}$  and the third term a quartic interaction potential for the scalar fields. The kinetic term for the four-dimensional Majorana fermion decomposes in a two-dimensional kinetic part and a Yukawa interaction between the Majorana fermion  $\lambda$  and the scalar fields  $\phi_m$ ,

$$\bar{\lambda}\Gamma^M D_M\lambda = \bar{\lambda}\Gamma^\mu D_\mu\lambda - ig\bar{\lambda}\Gamma^{m+1}[\phi_m, \lambda]. \quad (2.11)$$

Note, that the four-component Majorana spinor  $\lambda$  turns into two (real) Majorana spinors in two dimensions (in two dimensions an irreducible spinor has two components only). Later we will merge them into one complex two-component Dirac spinor. After rescaling all fields  $A, \lambda$  and  $\phi$  according to  $A \rightarrow g^{-1}A$  and absorbing afterwards the volume of the compactified torus in the gauge coupling  $1/g^2 \rightarrow V_{\mathcal{T}}/g^2$ , we obtain the action of the two-dimensional

$\mathcal{N} = (2, 2)$  SYM theory

$$S = \frac{1}{2g^2} \int d^2x \operatorname{tr} \left\{ -\frac{1}{2} F_{\mu\nu} F^{\mu\nu} + i\bar{\lambda} \Gamma^\mu D_\mu \lambda + D_\mu \phi_m D^\mu \phi_m + \bar{\lambda} \Gamma^{m+1} [\phi_m, \lambda] + \frac{1}{2} [\phi_m, \phi_n] [\phi^m, \phi^n] \right\}, \quad (2.12)$$

the Euclidean version of which we use in our lattice simulations. In a next step we combine the four-components of the Majorana spinor  $\lambda$  in two components of an irreducible Dirac spinor in two dimensions and rewrite the action in terms of Dirac fermions and complex scalars. Then the symmetries of the model are transparent and we can easily compare with the  $\mathcal{Q}$ -exact formalism [31]. With the Ansatz

$$\lambda = \sum_{r=1}^2 e_r \otimes \chi_r \quad \Longrightarrow \quad \bar{\lambda} = \sum_{r=1}^2 e_r^T \otimes \bar{\chi}_r, \quad (2.13)$$

where  $\{e_1, e_2\}$  is a Cartesian basis of  $\mathbb{R}^2$ , on which  $\Gamma^0$  in (2.8) acts trivially, and  $\chi_r$  are irreducible Majorana spinors in two dimensions, we obtain

$$S = \frac{1}{2g^2} \int d^2x \operatorname{tr} \left\{ -\frac{1}{2} F_{\mu\nu} F^{\mu\nu} + D_\mu \phi_m D^\mu \phi_m + \frac{1}{2} [\phi_m, \phi_n] [\phi_m, \phi_n] + i\bar{\chi}_r \gamma^\mu D_\mu \chi_r - \bar{\chi}_r (i\sigma_1)^{rs} \gamma_5 [\phi_1, \chi_s] - \bar{\chi}_r (i\sigma_3)^{rs} \gamma_5 [\phi_2, \chi_s] \right\} \quad (2.14)$$

that contains two flavours  $\chi_r$  of Majorana fermions and two real scalar fields. Introducing the Dirac fermion  $\psi$  and the complex scalar  $\varphi$  according to

$$\psi = \frac{1}{\sqrt{2}} (\chi_1 + i\gamma_5 \chi_2), \quad \bar{\psi} = \frac{1}{\sqrt{2}} (\bar{\chi}_1 + i\bar{\chi}_2 \gamma_5), \quad \varphi = \phi_1 + i\phi_2, \quad (2.15)$$

we end up with

$$S = \frac{1}{g^2} \int d^2x \operatorname{tr} \left\{ -\frac{1}{4} F_{\mu\nu} F^{\mu\nu} + \frac{1}{2} (D_\mu \varphi)^\dagger (D^\mu \varphi) - \frac{1}{8} [\varphi^\dagger, \varphi]^2 + i\bar{\psi} \gamma^\mu D_\mu \psi - \bar{\psi} P_+ [\varphi, \psi] - \bar{\psi} P_- [\varphi^\dagger, \psi] \right\} \quad (2.16)$$

with chiral projection operators  $P_\pm = (1 \pm \gamma_5)/2$ . When proving this results one may use that for two Majorana spinors  $\chi_1, \chi_2$  the trace of  $\bar{\chi}_1 [\varphi, \chi_2] + \bar{\chi}_2 [\varphi, \chi_1]$  vanishes. Under dimensional reduction, the four-dimensional Lorentz transformations in  $SO(1, 3)$  turn into two-dimensional Lorentz transformations and flavour rotations for the scalar fields ( $R$  symmetry), i.e.

$$SO(1, 3) \rightarrow SO_L(1, 1) \times SO_R(2), \quad (2.17)$$

and correspondingly  $Spin(1, 3)$  turns into  $Spin(1, 1)$  and  $R$ -transformations of the two spinor

fields, generated by  $\Sigma_{23} = -\sigma_3 \otimes \mathbb{1}/2$ . This  $R$ -symmetry acts on the real fields as

$$\begin{pmatrix} \phi_1 \\ \phi_2 \end{pmatrix} \rightarrow R(2\alpha) \begin{pmatrix} \phi_1 \\ \phi_2 \end{pmatrix}, \quad \begin{pmatrix} \chi_1 \\ \chi_2 \end{pmatrix} \rightarrow R(-\alpha) \begin{pmatrix} \chi_1 \\ \chi_2 \end{pmatrix}, \quad (2.18)$$

where  $R(\alpha)$  is a rotation with angle  $\alpha$ . The complex fields transform as

$$\varphi \rightarrow \exp(2i\alpha)\varphi, \quad \psi \rightarrow \exp(-i\alpha\gamma_5)\psi, \quad \bar{\psi} \rightarrow \bar{\psi}\exp(-i\alpha\gamma_5), \quad (2.19)$$

which is identified as chiral symmetry in two dimensions. In contrast, the four-dimensional chiral symmetry turns into a phase rotation of the Dirac field,

$$\lambda' = \exp(i\alpha\Gamma_5)\lambda = \begin{pmatrix} \cos\alpha & \gamma_5\sin\alpha \\ -\gamma_5\sin\alpha & \cos\alpha \end{pmatrix} \begin{pmatrix} \lambda_1 \\ \lambda_2 \end{pmatrix} \Rightarrow \psi' = \exp(-i\alpha)\psi \quad (2.20)$$

and implies fermion number conservation in two dimensions. This observations allow us to introduce two different fermion mass terms in the lattice formulation with Wilson fermions. A four-dimensional Majorana mass term proportional to  $\bar{\lambda}\lambda$  which violates fermion number conservation in two dimensions or a two-dimensional Dirac mass term  $\bar{\psi}\psi$  which violates chiral symmetry. When fine tuning to the supersymmetric continuum limit we shall break chiral symmetry of the reducible model in order to have the same fermionic symmetries as in the  $\mathcal{Q}$ -exact formulation in [32], to which we shall compare our results.

## 2.1 Expected mass spectrum

Veneziano and Yankielowicz where the first to derive a low energy effective Lagrangian for  $\mathcal{N} = 1$  SYM theory in four dimensions, in analogy to QCD [4]. They conjectured that the lightest super-multiplet contains the bound states shown in Table 1(a): a scalar meson a-f,

particle	spin	name	particle	spin	name
$\bar{\lambda}\gamma_5\lambda$	0	a- $\eta$	$F^{MN}F_{MN}$	0	0 <sup>++</sup> glueball
$\bar{\lambda}\lambda$	0	a-f	$F^{MN}\epsilon_{MNRST}F^{RS}$	0	0 <sup>-+</sup> glueball
$F_{MN}\Sigma^{MN}\lambda$	$\frac{1}{2}$	gluino-glueball	$F_{MN}\Gamma^M D^N\lambda$	$\frac{1}{2}$	gluino-glueball

(a) VY multiplet (b) FGS multiplet

**Table 1:** Multiplet structure of  $\mathcal{N} = 1$  SYM theory as predicted by low energy effective actions [4, 6].

a pseudoscalar meson a- $\eta$  and a spin 1/2 bound state between a Majorana fermion and a gauge boson, called gluino-glueball. We refer to this super-multiplet as the VY-multiplet. In a confining theory one also expects glueballs in the particle spectrum. Therefore a second super-multiplet was added by Farrar, Gabadadze and Schwetz [6]. The FGS-multiplet is shown in Table 1(b). It contains a scalar glueball, a pseudoscalar glueball as well as a spin 1/2 gluino-glueball. Predictions about the mass-hierarchy of the two multiplets vary in the literature [4–7]. In four dimensions large scale Monte-Carlo simulations with

Wilson fermions have been performed to investigate the spectrum of bound states [19]. The formation of the VY-multiplet containing both mesons and a gluino-gluonball has been observed while the  $0^{-+}$  gluonball is significantly heavier. Within (large) errors the  $0^{++}$  gluonball has the same mass as the  $f$  meson, but due to mass mixing, it is not clear whether the operator projects onto the correct state. Thus the formation of a heavier multiplet has not been confirmed yet.

The multiplet structure of the  $\mathcal{N} = (2, 2)$  SYM model can be extracted either from an effective Lagrangian of the two-dimensional system or by dimensionally reducing the supermultiplets of the four-dimensional effective theory. Thereby one should be cautious since the reduced model should contain massless states [26] and a super-multiplet with massless

particle	spin	name
$\bar{\lambda}\Gamma_5\lambda$	0	a- $\eta$
$\bar{\lambda}\lambda$	0	a-f
$F_{\mu\nu}\Sigma^{\mu\nu}\lambda + 2i[\phi_1, \phi_2]\Sigma^{23}\lambda$	$\frac{1}{2}$	gluino-gluon/scalarball

particle	spin	name
$[\phi_1, \phi_2]F_{\mu\nu}$	0	gluon-scalarball
$F_{\mu\nu}F^{\mu\nu} - 2D_\mu\phi_m D^\mu\phi_m - 2[\phi_1, \phi_2]^2$	0	$0^{++}$ -gluonball, scalarball
$F_{\mu\nu}\Gamma^\mu D_\nu\lambda - D_\mu\phi_m (i\Gamma^\mu[\phi^m, \lambda] + \Gamma^{m+1}D^\mu\lambda) - [\phi_m, \phi_n]\Gamma^{m+1}[\phi^n, \lambda]$	$\frac{1}{2}$	gluino-gluon/scalarball

**Table 2:** Two dimensional reduced supermultiplets for the  $N = (2, 2)$  theory. In the main body of the text we will call  $F_{\mu\nu}\Sigma^{\mu\nu}\lambda$  the gluino-gluonball and  $[\phi_1, \phi_2]\Sigma^{23}\lambda$  the gluino-scalarball.

states looks different as a massive super-multiplet. Thus it is not straightforward to foresee the multiplet structure of the reduced system. In any case, the expected bound states – massive or massless – of the  $\mathcal{N} = (2, 2)$  SYM model are listed in Table 2.

## 2.2 Supersymmetry restoration in the continuum limit

As argued in the introduction, the lattice will break supersymmetry explicitly. To restore it in the continuum limit, we have to fine-tune all relevant supersymmetry breaking operators that are allowed by the remaining symmetries on the lattice. For  $\mathcal{N} = (2, 2)$  SYM, a discussion of supersymmetry breaking operators is contained in [32]. Thereby the authors use a lattice formulation where one nilpotent supersymmetry is exactly preserved on the lattice. In contrast, in our lattice formulation with Wilson fermions the operator  $\phi^2$  may show up in the effective action. To cancel this term we must introduce a scalar mass counterterm  $m_s^2\phi^2$  that has to be fine-tuned. The fine-tuned continuum value  $m_s^2 = 0.65948255(8)$  has been calculated to one-loop order (which is sufficient for this theory) in [22]. Although a formulation with compact scalar fields has been used, we checked that this value is also correct for non-compact scalar fields used in our simulation. This can be explained as

follows: The Jacobian of the transformation from the compact variables in [22] to non-compact variables cancels (in one-loop) the additional contribution in the action for the compact fields. Thus we find the identical continuum value for  $m_s^2$  in both formulations.

As for the four-dimensional mother-theory there is only one relevant susy breaking term in two dimensions. Because of the similarity of the two theories one expects an important role of the fermion mass term in two dimensions as well. Let us first recall the impact of a fermion mass in four dimensions. Calculating the Ward identities for the chiral symmetry and the supersymmetry on the lattice, Curci and Veneziano demonstrated that only the renormalized gluino mass will appear as a relevant additional lattice contribution in the Ward identities [8]. Therefore by fine-tuning the bare gluino mass (in our case the fermion mass), one recovers chiral symmetry and supersymmetry in the same limit. We expect the same mechanism to be at work in two dimensions and thus will fine-tune the fermion mass. Note that this idea is in line with [32], as the fermion mass must vanish in the continuum limit to recover the chiral limit, as it is not a relevant operator. A fine-tuning on the lattice will act as an improvement, reducing further supersymmetric violating contributions for finite lattice spacing.

### 2.3 Euclidean formulation

Since we can not simulate a model with Minkowski spacetime, we must construct a continuation to the corresponding Euclidean theory. This continuation for theories with Majorana fermions was discussed in [53–55]. In contrast to Dirac fermions there is only one Majorana spinor with  $\bar{\lambda} = \lambda^\top \mathcal{C}$ . One cannot impose the reality condition  $\bar{\lambda} = \lambda^\dagger$ . The action picks up an overall negative sign leading to

$$S = \int d^4x \mathcal{L}, \quad \mathcal{L} = \text{tr} \left( \frac{1}{4} F_{MN} F^{MN} - \frac{i}{2} \bar{\lambda} \Gamma^M D_M \lambda \right) \quad (2.21)$$

with Euclidean Gamma-matrices  $\Gamma_M$ . Majorana fermions exist in the dimensionally reduced Euclidean theory. As convenient representation we may use

$$\Gamma_\mu = \mathbb{1} \otimes \gamma_\mu, \quad \Gamma_2 = \sigma_1 \otimes \gamma_5, \quad \Gamma_3 = \sigma_3 \otimes \gamma_5, \quad \Gamma_5 = -\sigma_2 \otimes \gamma_5, \quad (2.22)$$

now with Euclidean  $\gamma_\mu$ . The hermitean matrices  $\Gamma_5 = \Gamma_0 \Gamma_1 \Gamma_2 \Gamma_3$  and  $\gamma_5 = i\gamma_0 \gamma_1$  are related as  $\Gamma_5 = -\sigma_2 \otimes \gamma_5$ . Rescaling the fields and absorbing the volume of the torus in a dimensionful gauge coupling the Lagrangian of the reduced Euclidean model reduces to

$$\mathcal{L} = \frac{1}{2g^2} \text{tr} \left\{ \frac{1}{2} F_{\mu\nu}^2 + (D_\mu \phi_m)^2 - \frac{1}{2} [\phi_m, \phi_n]^2 - i \bar{\lambda} \Gamma^\mu D_\mu \lambda - \bar{\lambda} \Gamma^{m+1} [\phi_m, \lambda] \right\}. \quad (2.23)$$

In terms of complex fields  $\psi$  and  $\varphi$  it takes the form

$$\mathcal{L} = \frac{1}{g^2} \text{tr} \left\{ \frac{1}{4} F_{\mu\nu}^2 + \frac{1}{2} (D_\mu \varphi)^\dagger (D^\mu \varphi) + \frac{1}{8} [\varphi^\dagger, \varphi]^2 - i \bar{\psi} \gamma^\mu D_\mu \psi + i \bar{\psi} P_+ [\varphi, \psi] + i \bar{\psi} P_- [\varphi^\dagger, \psi] \right\}. \quad (2.24)$$

In actual simulations we choose the formulation (2.23) with two real scalar fields and a reducible four-component Majorana spinor.

## 2.4 Ward identities

In order to check for the restoration of supersymmetry in the continuum limit, we monitor supersymmetric Ward identities

$$\langle \mathcal{Q}\mathcal{O} \rangle = 0, \quad (2.25)$$

with supercharge  $\mathcal{Q}$  introduced in (2.4) and operators  $\mathcal{O}$ . In four dimensions the fermionic operator

$$\mathcal{O}_a(x) = \text{tr}_c \left\{ \bar{\lambda}_b(x) (\Gamma^{MN})^b{}_a F_{MN}(x) \right\} \quad (2.26)$$

is frequently used and gives rise to the bosonic Ward identity

$$\frac{1}{V} \langle S_B \rangle = \langle \mathcal{L}_B \rangle = \frac{1}{4} \langle \text{tr} F^{MN} F_{MN} \rangle = -\frac{3}{8} \frac{i}{2} \langle \text{tr} \bar{\lambda} \not{D} \lambda \rangle = \frac{3}{2} (N_c^2 - 1) = \frac{9}{2}. \quad (2.27)$$

We made use of the fact that the expectation values of densities do not depend on  $x$ . Note that in the on-shell formulation, one obtains the factor of  $\frac{3}{8}$  instead of the factor  $\frac{1}{2}$  in the off-shell formulation [47]. The identity relates the expectation values of the bosonic part of the action to the fermionic part.

In accordance with the dimensional reduction we decompose the operator (2.26) into three terms: one with  $\{M, N\}$  being  $\{m, n\}$ , one with  $\{\mu, \nu\}$  and finally one with  $\{m, \mu\}$  or  $\{\mu, m\}$ . The corresponding three (two-dimensional) Ward identities read

$$\begin{aligned} W_1 &= \frac{1}{2} \langle [\phi_1, \phi_2]^2 \rangle - \frac{i}{8} \langle \bar{\lambda} \Gamma_2 [\phi_1, \lambda] + \bar{\lambda} \Gamma_3 [\phi_2, \lambda] \rangle = 0, \\ W_2 &= \frac{1}{4} \langle F_{\mu\nu} F^{\mu\nu} \rangle + \frac{i}{8} \langle \bar{\lambda} \Gamma_2 [\phi_1, \lambda] - \bar{\lambda} \Gamma_3 [\phi_2, \lambda] \rangle = \frac{3}{2}, \\ W_3 &= \frac{1}{2} \langle D_\mu \phi^m D^\mu \phi_m \rangle = 3. \end{aligned} \quad (2.28)$$

Note that the sum rule  $W_1 + W_2 + W_3$  just reproduces the result  $\frac{9}{2}$  in (2.27).

## 3 Lattice formulation

In the simulations we use Wilson fermions and the tree-level improved Lüscher-Weisz gauge action [56]. The scalar fields are treated as non-compact site-variables in the adjoint representation of the gauge group. The action for the scalar fields is implemented by using the forward difference

$$D_\mu^f \phi_x = \phi_{x+e_\mu} - U_{x,\mu}^A \phi_x \quad (3.1)$$

in the kinetic term, where the link variables  $U_{x,\mu}^A$  are in the adjoint representation. The fermion operator for Wilson fermions is then

$$D_{xy} = (m_f + 2 + \Gamma_{m+1} f^a \phi_a^m) \delta_{x,y} - \frac{1}{2} \sum_\mu (\mathbb{1} - \Gamma_\mu) \delta_{x+e_\mu,y} U_{x,\mu}^A + (\mathbb{1} + \Gamma_\mu) \delta_{x-e_\mu,y} U_{y,\mu}^A{}^\top \quad (3.2)$$

where the matrices  $(f^a)_{bc}$  are the structure constants of the gauge group  $SU(2)$ . Integration over the Majorana fermion yields the Pfaffian of  $CD$  and we obtain for the partition function as integral over the bosonic fields,

$$Z = \int \mathcal{D}U \mathcal{D}\phi \text{Sign}(\text{Pf}(CD)) \det(D^\dagger D)^{\frac{1}{4}} e^{-S[U, \phi]}. \quad (3.3)$$

We made use of the  $\Gamma_5$ -hermiticity of the fermion operator  $\Gamma_5 D \Gamma_5 = D^\dagger$ . The fourth root of  $D^\dagger D$  is approximated by a rational approximation in the rHMC [57–60] algorithm.

### 3.1 Sign problem and flat directions

Two known problems may potentially spoil the Monte-Carlo simulations: a potential sign problem introduced by the Pfaffian and possible *flat directions* in which the scalar potential is constant. We address both issues in turn. Although the eigenvalues  $\lambda_i$  of the hermitian matrix  $Q = \Gamma_5 D$  are real and doubly degenerate [12], the Pfaffian can still introduce a sign problem that we have to take into account in the simulations. Using the dependence of the Pfaffian on the hopping parameter  $\kappa = 1/(2m_f + 4)$  it is possible to show [15] that the Pfaffian and the determinant are related by

$$\det D = \prod_i \lambda_i^2 \quad \Rightarrow \quad \text{Pf}(CD[U]) = \prod_i \lambda_i. \quad (3.4)$$

We use the nice spectral flow method introduced in [15] to monitor a potential sign problem. The idea is that for a given gauge field configuration (a typical one for fixed  $\beta$  and  $\kappa$ ) the eigenvalues  $\lambda_i$  vary continuously when the hopping parameter  $\kappa_{\text{spec}}$  in the fermion operator increases. For the free operator with  $\kappa_{\text{spec}} = 0$  the Pfaffian is positive. Therefore, the Pfaffian can only become negative if an odd number of eigenvalues  $\lambda_i(\kappa_{\text{spec}})$  change their signs as a function of  $\kappa_{\text{spec}}$ . We have monitored the 10 eigenvalues with smallest absolute values, shown in the left panel of Figure 1 for configurations generated with  $\beta = 17$  and  $\kappa = 0.26062$  as function of the flow parameter  $\kappa_{\text{spec}}$  increasing from 0 to the value of interest  $\kappa$ . The positive eigenvalues decrease monotonously while the negative eigenvalues increase as  $\kappa_{\text{spec}} \rightarrow \kappa$ , but they do not cross zero such that the Pfaffian for this configuration remains positive. Furthermore we show the smallest eigenvalues for three ensembles of 1000 gauge configurations each belonging to the three flow parameters  $\kappa_{\text{spec}} = \kappa, 0.25734, 0.25520$  in Figure 1. Even for  $\kappa_{\text{spec}} = \kappa$  no eigenvalue is small enough to change its sign. Hence the sign of the Pfaffian is always positive. We repeated the simulation for different volumes, inverse gauge couplings and hopping parameters. For  $\kappa < \kappa_c$  we never observed a negative Pfaffian while for  $\kappa > \kappa_c$  approximately one in thousand configurations had a negative sign. Thus we safely conclude that there is no sign problem in our simulations.

The scalar potential

$$V[\phi_1, \phi_2] = [\phi_1, \phi_2]^2 \quad (3.5)$$

in the bosonic action is invariant under a shift

$$\phi_1 \rightarrow \phi_1 + \alpha \phi_2 \quad \phi_2 \rightarrow \phi_2, \quad (3.6)$$

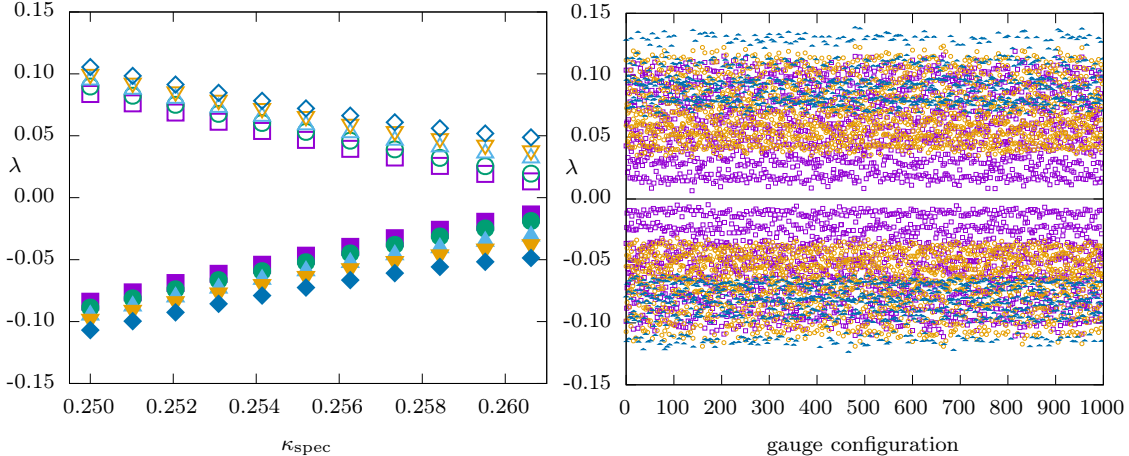


**Figure 1:** Left: Spectral flow of 10 eigenvalues with smallest absolute values for  $\beta = 17$ ,  $\kappa = 0.26062$  on a  $64 \times 32$  lattice. Right: Smallest eigenvalues for three different values of the spectral flow parameter  $\kappa_{\text{spec}}$ : 0.25520 (blue triangles), 0.25734 (orange circles) and  $\kappa$  (purple squares).

where  $\alpha$  is an arbitrary real parameter. This is an example of a *flat direction* in the space of fields  $(\phi_1, \phi_2)$  along which the potential is constant. Flat directions are generic for SYM-theories with extended susy and may destabilize Monte-Carlo simulations since the scalar fields may escape along these directions. Flat directions may either be lifted dynamically by quantum corrections or explicitly by introducing a mass term  $m_s^2 \phi^2$ . Actually, as emphasized earlier, on the lattice we *must* introduce a mass term with finite  $m_s$  to find the correct supersymmetric continuum limit. This term (which is needed even for  $a \rightarrow 0$ ) lifts the flat directions explicitly. This is shown in Figure 2 where we plotted the spatial average  $\overline{\phi^2} = \frac{1}{V} \sum \phi_x^2$  as function of Monte-Carlo time for  $\beta = 17$ ,  $\kappa = 0.26178$  on a  $64 \times 32$  lattice in the left panel and the expectation value of  $\overline{\phi^2}$  as function of  $m_s$  in the right panel. For all sets of parameters considered, the absolute value of the scalar fields does not run away. Hence we conclude, that flat directions are lifted for values  $m_s$  near the value of the supersymmetric model and thus cause no problems in the simulations. In a previous work the lifting of flat directions has been observed even for the susy-breaking value  $m_s^2 = 0$  and small values of the inverse gauge coupling [61].

### 3.2 Scalar and fermion mass fine tuning

The scalar mass is the only relevant coupling that has to be fine-tuned to restore supersymmetry in the continuum limit (in two dimensions the fermion mass needs not be fine tuned). Its value in the thermodynamic and continuum limit is analytically known from one-loop perturbation theory  $m_s^2 = 0.65948$  [22]. On the finite  $64 \times 32$  lattice the mass is shifted towards the smaller value  $m_s^2 = 0.62849$ . In order to investigate the dependence of expectation values on  $m_s^2$  we performed simulations for a larger range  $m_s^2 \in [0.50, 0.80]$ . Although the scalar mass breaks supersymmetry explicitly, it turns out that within the statistical uncertainties the Ward identities are independent of the scalar mass. Therefore we set the scalar mass to  $m_s^2 = 0.66$ , very close to the continuum value, in our simulations.

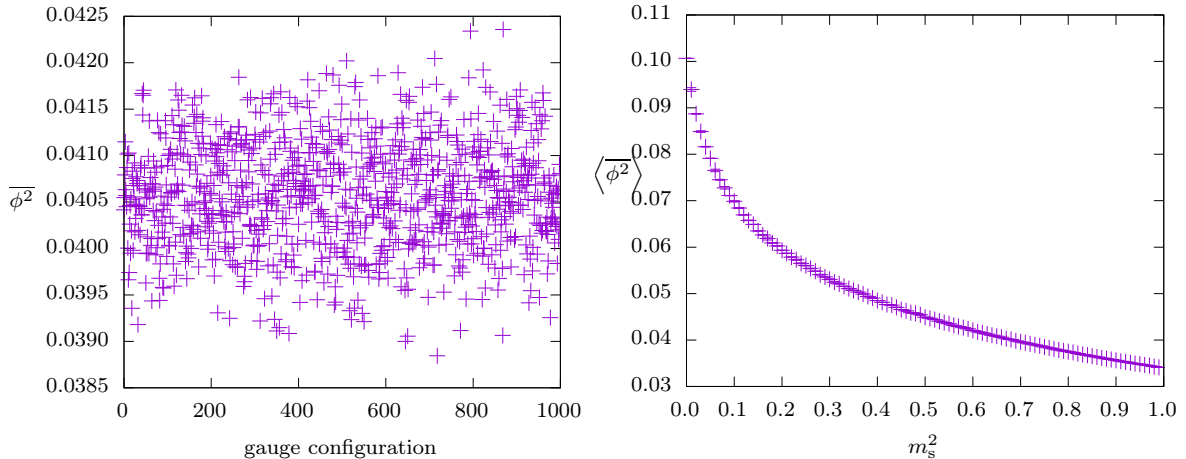


**Figure 2:** Spatial average of squared scalar field as function of Monte-Carlo time for  $\beta = 17$ ,  $\kappa = 0.26178$ ,  $m_s^2 = 0.66$  (left) and its expectation as function of  $m_s^2$  (right) on a  $64 \times 32$  lattice. The (one-loop) value for the fine-tuned explicit scalar mass at the supersymmetric point is  $m_s^2 \approx 0.6595$ .

In contrast to four-dimensional  $\mathcal{N} = 1$  SYM theory, a fine-tuning of the bare fermion mass  $m_f$  is not necessary to restore supersymmetry in the continuum limit. Nevertheless we shall enhance the chiral properties on the lattice by tuning  $m_f$  to its critical value  $m_f^c(L, \beta)$ , that depends on the inverse gauge coupling  $\beta$  but depends little on the lattice size. In the continuum limit, the critical fermion mass should approach  $m_f^c = 0$ , in agreement with the results in [22, 32]. There are two straightforward methods to determine the critical fermion mass on a finite lattice. The first uses the order parameter for chiral symmetry  $\langle \bar{\lambda} \lambda \rangle$  and defines  $m_f^c$  by the peak position of the chiral susceptibility. The second method comes from an analogy to QCD which is also employed in the four-dimensional  $\mathcal{N} = 1$  SYM theory [4, 16, 62]: Although the pion is not a physical particle in the theory, one can define its correlation function in a partially quenched setup which mimics a second Majorana flavour in  $\mathcal{N} = 1$  SYM. The pion mass is related to the renormalized gluino mass by

$$m_q \propto m_\pi^2. \quad (3.7)$$

We expect this relation to hold in two dimensions as well and define the critical fermion mass at the value where the gluino mass vanishes. The results for the two methods are given in Table 3. Both methods yield comparable values for the critical fermion mass. One observes that the fermion mass approaches the expected continuum value from below. In the following section we show that  $\sqrt{\beta} \propto a$ . Therefore we extrapolate our results to the continuum with the ansatz

$$m_f^c(\beta) = m_\infty + c_1 \beta^{-e_1} + c_2 \beta^{-e_2}. \quad (3.8)$$

The coefficients  $c_i$  encode lattice artifacts and in the continuum limit  $m_f^c(\beta \rightarrow \infty) = m_\infty$ . Since  $m_f^c(\beta)$  does not depend significantly on the lattice size, we also include simulations

$\beta$	14.0	15.5	17.0	18.0	19.0
$m_f^c(\chi_s)$	-0.0983(2)	-0.0969(4)	-0.0896(22)	-0.0857(6)	-0.0819(4)
$m_f^c(\pi)$	-0.1003(1)	-0.0931(1)	-0.0853(1)	-0.0821(1)	-0.0787(1)
$\beta$	40	60	80	100	
$m_f^c(\pi)$	-0.0413(5)	-0.0272(5)	-0.0243(7)	-0.0189(4)	

**Table 3:** Critical fermion mass  $m_f^c$  for different  $\beta$ . To determine the mass we use the chiral susceptibility and the mass of the pion ground state.

at  $\beta = 40, 60, 80, 100$  on smaller lattices into the extrapolation. The results of the fits are shown in Table 4. We give two different values  $\chi_w^2$  and  $\chi^2$  for the goodness of the fit. The first  $\chi_w^2$  was calculated including the errors for  $m_f^c$  as weights in the fit and the second  $\chi^2$  without weights.  $\chi^2$  is much smaller, showing that the fit of the given ansatz to the data is very good, but the errors for the critical masses are probably underestimated<sup>1</sup>. Within uncertainties the values for  $m_\infty$  are compatible with the expected results  $m_\infty = 0$ .

$m_\infty$	$c_1$	$c_2$	$e_1$	$e_2$	$\chi_w^2$	$\chi^2$
0.0108(9)	-0.218(9)	-0.74(2)	<u>1/2</u>	<u>1</u>	18.98	$1.25 \times 10^{-6}$
-0.0037(4)	-1.59(1)	3.27(13)	<u>1</u>	<u>2</u>	21.85	$8.77 \times 10^{-7}$
0.0037(8)	-0.83(1)	<u>0</u>	0.785(8)	-	19.04	$1.11 \times 10^{-6}$

**Table 4:** Fit values for the fit function given in (3.8), for three different sets of parameters. The mass  $m_\infty$  represents the continuum value of the critical fermion mass  $m_f^c$ , which should be zero. The underlined parameters are prescribed in the 2-parameter fits.

### 3.3 Scale setting and lattice spacing

In order to determine the lattice spacing and perform the continuum limit, we consider the static quark-antiquark potential in the fundamental representation of SU(2) and extrapolate with the expected form

$$V(r) = A + \frac{C}{r} + \sigma r \quad (3.9)$$

to the chiral limit. Here  $C$  parametrizes the Coulomb term and  $\sigma$  is the string tension. For  $\beta = 17$  and  $m_f = -0.044$  the potential is shown in Figure 3. To compare our results to usual QCD lattice data, we employ the Sommer scale [63] and define a lattice spacing in physical units. The results for three different values of the inverse gauge coupling

$$\beta = \frac{1}{a^2 g^2} \quad (3.10)$$

<sup>1</sup>The errors given for the critical fermion masses  $m_f^c$  include only fit errors but not statistical errors.

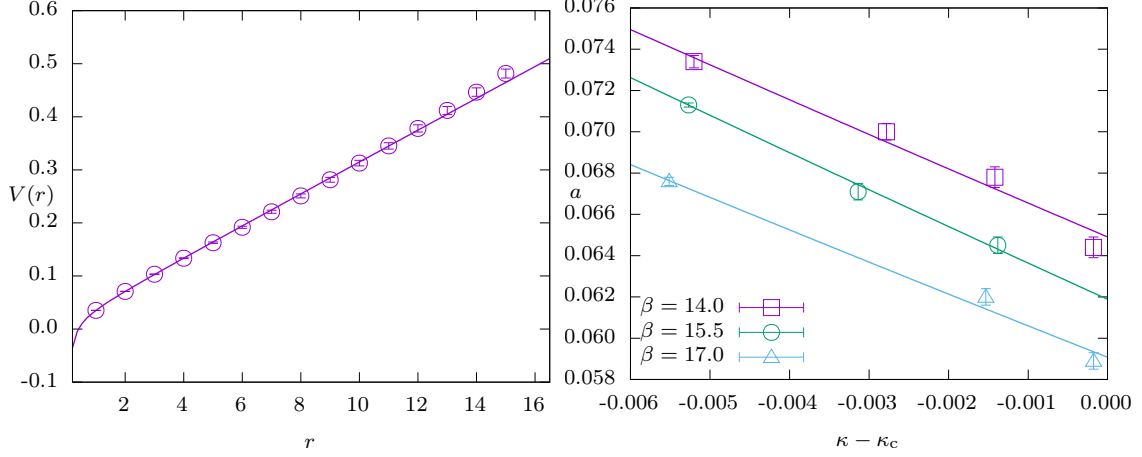


**Figure 3:** Left: Static quark potential and fit to (3.9) for  $\beta = 17.0$  and  $m_f = -0.044$ . Right: Lattice spacing  $a$  for  $\beta = 14.0, 15.5$  and  $17.0$  as function of  $\kappa$  on a  $64 \times 32$  lattice.

are depicted in Table 5. Since the lattice spacing  $a$  heavily depends on the fermion mass, we extrapolate the latter to its chiral limit  $m_f = m_f^c$ . The results are given in Table 5. In the last rows we checked that the inverse dimensional coupling  $1/g^2 = \beta a^2$  in (3.10) is almost independent of  $\beta$ , confirming that the continuum limit is reached for  $\beta \rightarrow \infty$ .

$\beta = 14.0$					
$m_f$	-0.062	-0.08	-0.09	-0.099	-0.100
$a[\text{fm}]$	0.0734(3)	0.0700(4)	0.0678(5)	0.0644(5)	0.0650(25)
$\beta a^2[\text{fm}]$	0.0754(6)	0.0686(8)	0.0644(9)	0.0581(9)	0.0592(46)
$\beta = 15.5$					
$m_f$	-0.054	-0.07	-0.083		-0.093
$a[\text{fm}]$	0.0713(1)	0.0671(4)	0.0645(4)		0.0618(18)
$\beta a^2[\text{fm}]$	0.0788(2)	0.0698(8)	0.645(8)		0.0592(35)
$\beta = 17.0$					
$m_f$	-0.044	-0.074	-0.084		-0.085
$a[\text{fm}]$	0.0676(2)	0.0620(4)	0.0589(4)		0.0591(16)
$\beta a^2[\text{fm}]$	0.0777(5)	0.0653(8)	0.0590(8)		0.0595(31)

**Table 5:** Lattice spacing for different combinations of  $\beta$  and  $m_f$ . In the last column we give the extrapolations to the chiral limit.

### 3.4 Smearing

We use three different kinds of smearing in the simulations. For the scalar fields we utilize the low pass filter for functions. This smearing process is defined as

$$\tilde{\phi}^n(x) = (1 + \epsilon\Delta)\tilde{\phi}^{n-1}(x) \quad \text{with} \quad \tilde{\phi}^0(x) = \phi(x), \quad (3.11)$$

where  $\phi(x)$  is the scalar field,  $\tilde{\phi}^n(x)$  is the smeared field and  $\epsilon$  is the smearing parameter. For gauge fields we use STOUT smearing [64] and for the fermionic sinks and sources on the lattice we apply Jacobi smearing [65, 66].

$\beta$	$m_f$	$m_s^2$	# C	$\beta$	$m_f$	$m_s^2$	# C
14.0	-0.09900	0.66	20000	15.5	-0.08300	0.66	20000
14.0	-0.09675	0.66	15000	15.5	-0.07000	0.66	20000
14.0	-0.09450	0.66	15000	15.5	-0.05400	0.66	20000
14.0	-0.09225	0.66	15000	17.0	-0.08400	0.66	14000
14.0	-0.09000	0.66	20000	17.0	-0.08150	0.66	15000
14.0	-0.08000	0.66	20000	17.0	-0.07900	0.66	15000
14.0	-0.06200	0.66	20000	17.0	-0.07650	0.66	15000
15.5	-0.09200	0.66	20000	17.0	-0.07400	0.66	20000
15.5	-0.08975	0.66	15000	17.0	-0.06200	0.66	20000
15.5	-0.08750	0.66	15000	17.0	-0.04400	0.66	20000
15.5	-0.08525	0.66	15000				

**Table 6:** Number of Configurations (# C) for the given parameters  $\beta$ ,  $m_f$  and  $m_s$  on a  $64 \times 32$  lattice.

In Table 6 we give the number of configurations generated for the given sets of parameters  $\{\beta, m_f, m_s\}$  on a  $64 \times 32$  lattice. A large number of configurations is needed to extract the masses of the ground- and excited states of the f-meson. Large fluctuations of the two scalar fields entering the fermion operator via the Yukawa terms induce strong fluctuations of fermion correlators.

#### 4 Restoration of Ward identities

The simple continuum Ward identities (2.28) do not hold on the lattice since (in our formulation) there are just no supersymmetries which leave the lattice action invariant. But in the continuum limit we must recover these identities if we take the finite additive renormalization of the parameter  $m_s^2$  into account.

Inspired by the treatment of four-dimensional models in [8, 14, 67–69] we impose three rules to define the lattice transformations:

1. They become the continuum susy transformations in the continuum limit.
2. They commute with the gauge transformations.
3. The transformation of the covariant derivative is the lattice equivalent of the continuum counterpart.

These rules allow us to reduce the plethora of possible lattice transformations acting on the

lattice fields  $\{U_\mu(x), \lambda(x), \phi_m(x)\}$  to a small set. We choose the transformations

$$\begin{aligned}\bar{Q}^\alpha U_\mu(x) &= \frac{a}{2} U_\mu(x) (\Gamma_\mu)^\alpha{}_\beta \lambda^\beta(x + ae_\mu), & \bar{Q}^\alpha U_\mu^\dagger(x) &= -\frac{a}{2} (\Gamma_\mu)^\alpha{}_\beta \lambda^\beta(x + ae_\mu) U_\mu^\dagger(x), \\ \bar{Q}^\alpha \lambda_\beta &= 0, & \bar{Q}^\alpha \bar{\lambda}_\beta &= -(\Gamma_{\mu\nu})^\alpha{}_\beta G^{\mu\nu}, & \bar{Q}^\alpha \phi_m &= \frac{1}{2} \Gamma_{m+1}{}^\alpha{}_\beta \lambda^\beta,\end{aligned}\tag{4.1}$$

where all fields but  $U_\mu$  carry the canonical dimensions in four dimensions and  $a^2 G^{\mu\nu}$  is the clover plaquette. Since the lattice action is not invariant the continuum Ward identities are deformed to lattice identities

$$\langle \bar{Q}O \rangle = \langle O \bar{Q} S_{\text{lat}} \rangle, \tag{4.2}$$

where the transformation of the Lagrangian is given by

$$\bar{Q}^\alpha \mathcal{L}_{\text{lat}} = \frac{\beta}{2} \left\{ \partial_\mu s_\mu^\alpha - (m_f - m_f^c) \chi_f^\alpha + \left( m_s^2 - (m_s^c)^2 \right) \chi_s^\alpha \right\} + \mathcal{O}(a) \tag{4.3}$$

with dimensional quantities  $\mathcal{L}_{\text{lat}}$  and  $\beta$ . After summing over all lattice sites the contribution of the supercurrent  $s_\mu^\alpha$  vanishes, up to terms of order  $\mathcal{O}(a)$ . In addition, the terms  $\chi_f^\alpha$  and  $\chi_s^\alpha$  represent corrections introduced by a nonzero fermion mass  $m_f$  and a scalar mass  $m_s$  away from their critical values. These terms are suppressed after fine-tuning the masses. Details on the calculation are given in Appendix A. Finally we obtain the lattice Ward identities in the chiral limit  $m_f \rightarrow m_f^c$

$$\begin{aligned}W_B = \beta V^{-1} \langle S_B \rangle + \beta m_s^2 \langle \text{tr} \phi^2 \rangle &\rightarrow \frac{9}{2}, & W_3 = \frac{\beta}{2} \langle \text{tr} D_\mu \phi^a D^\mu \phi_a \rangle + \beta m_s^2 \langle \text{tr} \phi^2 \rangle &\rightarrow 3, \\ W_2 = \frac{\beta}{4} \langle \text{tr} F_{\mu\nu} F^{\mu\nu} \rangle + \beta \langle \text{tr} \bar{\lambda} \Upsilon \rangle &\rightarrow \frac{3}{2}, & W_1 = \frac{\beta}{2} \langle \text{tr} [\phi_1, \phi_2]^2 \rangle - \beta \langle \text{tr} \bar{\lambda} \Upsilon \rangle &\rightarrow 0,\end{aligned}\tag{4.4}$$

where we used the abbreviation

$$\Upsilon = \frac{i}{8} (\Gamma_2 [\phi_1, \lambda] + \Gamma_3 [\phi_2, \lambda]). \tag{4.5}$$

#### 4.1 Extrapolation to the chiral limit

For this analysis, we used additional lattices with parameters  $\beta = 40, 60, 80, 100$ ,  $L_T = 16$  and  $L_S = 8$ . Such small lattices are reasonable since the Ward identities show no dependence on the lattice size for  $L_{S,T} > 8$  for all  $\beta$ . To extrapolate our results to the chiral limit we need a guess for the functional dependence of the Ward identities on the bare mass  $m_f$ . In two dimensions there is no spontaneous symmetry breaking and correlators are smooth functions of  $m_f$ . Our simulations indicate that bosonic correlators show, up to an additive constant  $b$ , a smoothed step function behavior on the fermion mass. This motivates the following ansatz for their  $m_f$ -dependence near the *critical* fermion bare mass  $m_*$ :

$$W(m_f) \sim a \arctan \{ \xi (m_f - m_*) \} + b \tag{4.6}$$

with fit parameters  $a, b, m_*$  and  $\xi$ , where  $\xi$  is to be interpreted as lattice correlation length.

For example, in the left panel of Figure 4 we depicted fits to the Ward identity  $W_2$

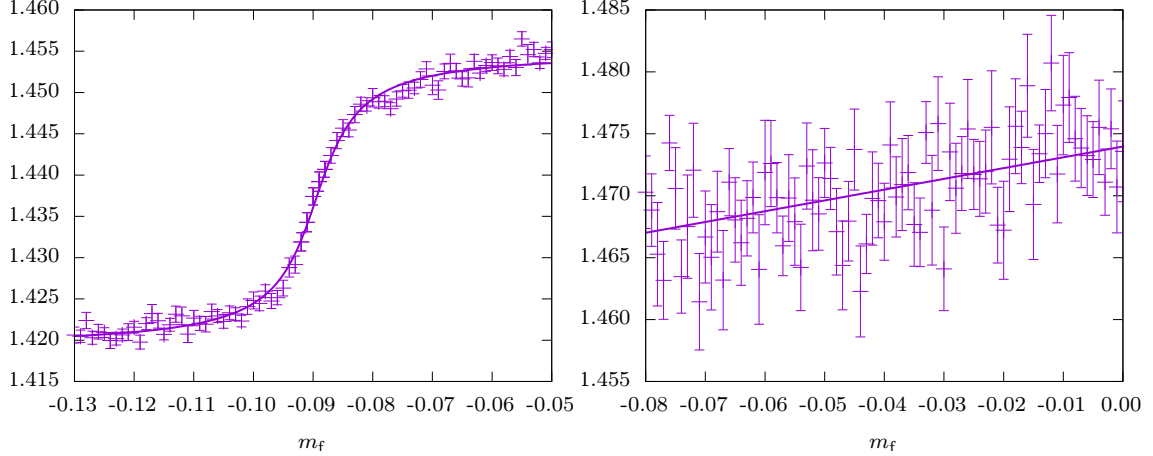


**Figure 4:** The Ward identity  $W_2$  in (4.4) is shown for  $\beta = 17$  (left) and  $\beta = 40$  (right).

which is dominated by the term quadratic in the field strength tensor. We observe that our ansatz yields a good approximation for the functional dependence of the data on  $m_f$ . The extracted value for  $m_*$  is very close to the critical fermion mass  $m_f^c$ . For  $\beta \gtrsim 40$  this ansatz is not appropriate anymore and we use a linear fit function, as seen on the right hand side of Figure 4. This allows us to extract the value of the Ward identities in the chiral limit. Finally we have to extrapolate the Ward identities to the continuum limit. In the Appendix A we show that close to its critical value in the continuum  $m_s^2 = 0.65948$  the results are insensitive to the scalar mass and we simulate at  $m_s^2 = 0.66$ . In Figure 5 we show the

Ward identity	$W_1$	$W_2$	$W_3$	$W_B$
$\beta = 14.0$	-0.0204(17)	1.4360(27)	3.01012(90)	4.4434(79)
$\beta = 15.5$	-0.0162(16)	1.4403(29)	3.01081(42)	4.4486(55)
$\beta = 17.0$	-0.0154(13)	1.4447(25)	3.01007(51)	4.4533(71)
$\beta = 40.0$	-0.00246(22)	1.4703(15)	3.00367(48)	4.4729(24)
$\beta = 60.0$	-0.00145(12)	1.4790(8)	3.00216(49)	4.4807(17)
$\beta = 80.0$	-0.00096(8)	1.47831(8)	3.00233(49)	4.4853(18)
$\beta = 100.0$	-0.00084(31)	1.4869(27)	3.00211(67)	4.4877(16)
$\beta \rightarrow \infty$ (Fit 1)	0.0058(4)	1.517(2)	2.9951(6)	4.5135(33)
$\beta \rightarrow \infty$ (Fit 2)	0.0019(2)	1.4929(8)	2.9999(4)	4.494(2)
$\beta \rightarrow \infty$ (Fit 3)	-0.0005(2)	1.505(10)	3.001(1)	4.51(2)
$\beta \rightarrow \infty$ (weighted average)	-0.0005(2)	1.505(12)	2.999(3)	4.506(10)
theor. value	0	$\frac{3}{2}$	3	$\frac{9}{2}$

**Table 7:** Ward identity values for different  $\beta$  and a lattice size of  $64 \times 32$ . In the last columns we show continuum extrapolations with three different fit functions and a weighted average as well as the theoretical value.

results for all four Ward identities for different  $\beta$ . We observe a monotonic convergence

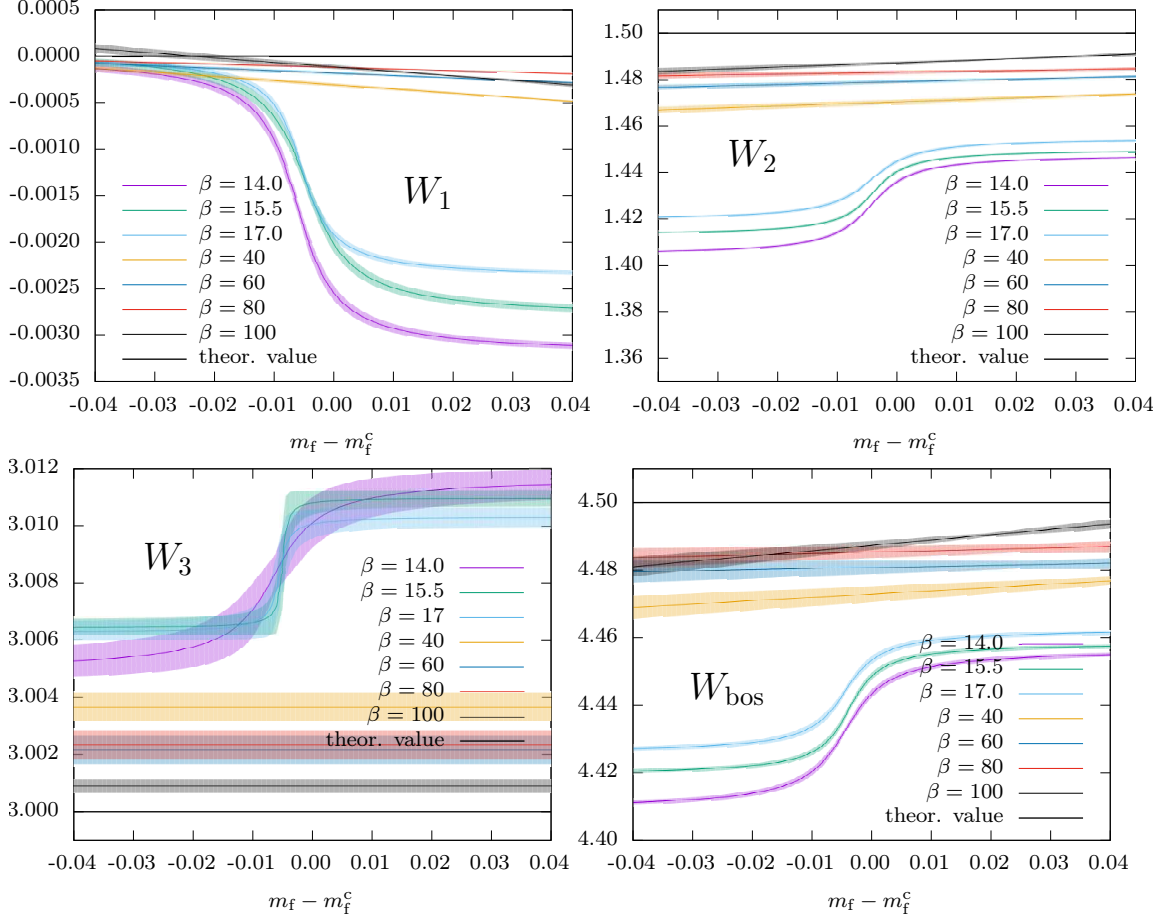


**Figure 5:** Ward identities (4.4) as functions of  $m_f - m_f^c$  with mean values and standard deviation (confident band) for various values of  $\beta$  between 14 and 100. Shown are the Ward identities  $W_1$  (top left),  $W_2$  (top right),  $W_3$  (bottom left) and the bosonic Ward identity. The analysis for the bosonic Ward identity  $W_B$  was done individually for the given data and is not the sum  $W_1 + W_2 + W_3$ .

to the expected continuum value. In Table 7 we give the values of all Ward identities for the chiral limit and different  $\beta$  together with the expected continuum value. The plots in Figure 6 show the dependence of the Ward identity on  $\beta$ . The Ward identities clearly converge to the supersymmetric continuum values. In order to extrapolate our results to the continuum limit, we use three different fits of the form

$$W(\beta) = W^\infty + b\beta^{-c} \quad (4.7)$$

with the prescribed value  $c = 1/2$  for Fit 1,  $c = 1$  for Fit 2 ( $b$  and  $W^\infty$  are free fit parameters). Fit 3 has three free fit parameters. The fits are shown in Figure 6 and the results for  $W^\infty$  are given in Table 7. From the three fit functions we can estimate a systematic error coming from the choice of a particular fit function. This error alleviates our bias in choosing such a function. The *weighted average* takes into consideration the

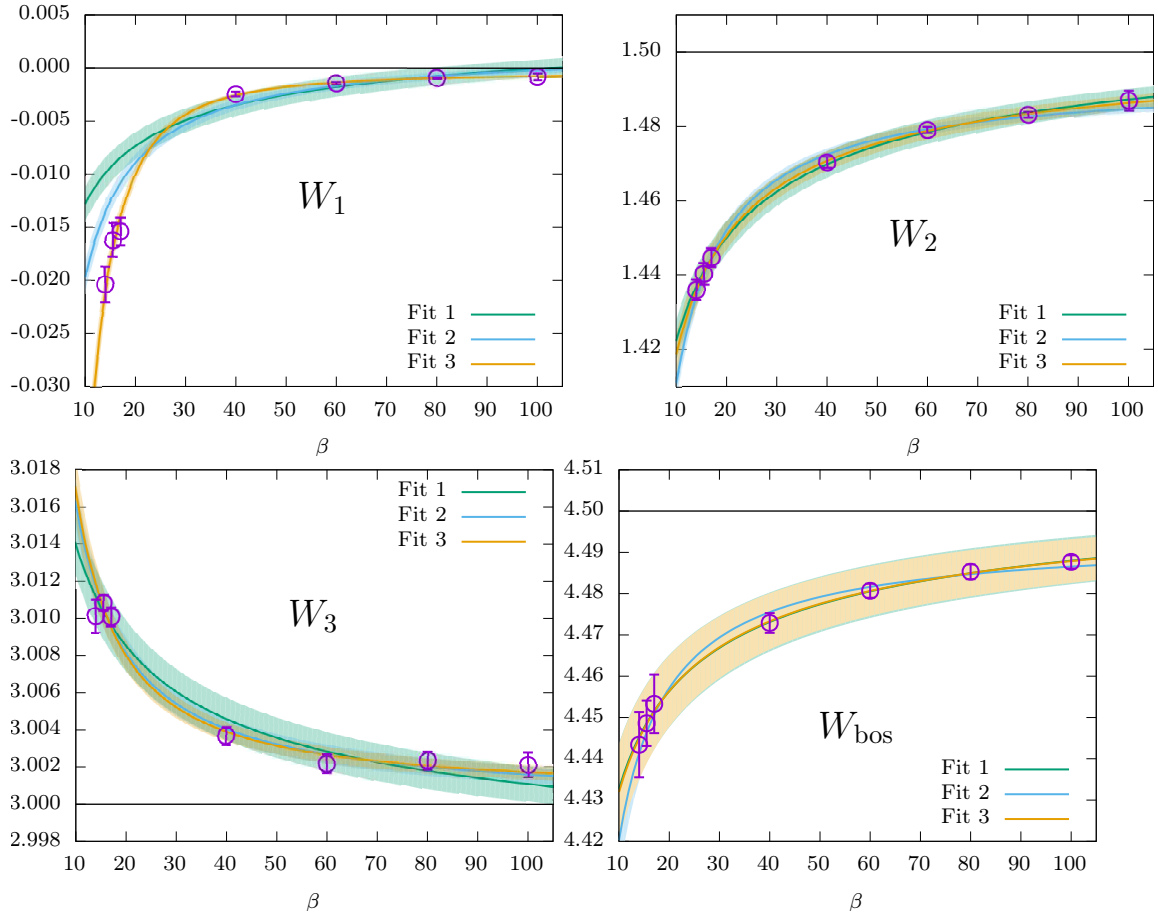


**Figure 6:** Ward identities for different values of  $\beta$  together with three different fits used for the continuum extrapolation. Horizontal lines indicate the theoretical value in the supersymmetric continuum limit.

goodness of the fits. The Ward identities clearly point to the restoration of supersymmetry in the continuum limit, indicating also no sign of spontaneous susy breaking.

## 5 Mass spectrum

In order to determine the mass spectrum of the theory, we first perform the infinite volume limit, then the chiral limit and finally the continuum limit. For the infinite volume limit we study the dependence of the mass of the lightest state on the size of the system in order to locate a  $\kappa$ - and  $\beta$ -range where the results are (almost) insensitive to the volume. Then we simulate the theory at a fixed lattice volume for different values of the hopping parameter  $\kappa$  and extrapolate the results to the critical value  $\kappa_c(\beta)$ , where the gluino becomes massless. Finally we repeat the simulations for three different values of the gauge coupling  $\beta$  and try to extrapolate the results to  $\beta \rightarrow \infty$ .

## 5.1 Volume dependence

The finite volume dependency of bound states is given by [70, 71]

$$m_L = m - \frac{c}{L} \exp\left(-\frac{L}{L_0}\right), \quad (5.1)$$

where  $m_L$  is the mass at a finite lattice with spatial length  $L$  and  $m$  the mass in the infinite volume limit. The parameter  $L_0$  represents the scale at which finite volume effects set in. In order to eliminate this fit parameter, we relate it to the infinite volume mass of the lightest particle, i.e.  $L_0 = \pi/m_\eta$ . For the fit we consider only masses  $m_L \geq \pi/L_t$ . The  $\eta$ -meson ground state mass  $m_L$  is shown for  $\beta = 12$  and four different values of  $\kappa$  in Figure 7. For

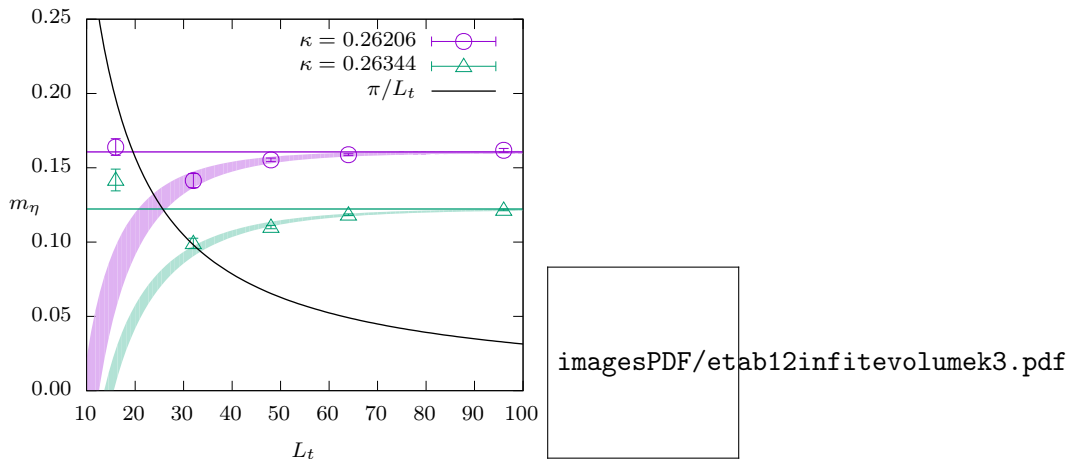


**Figure 7:** Infinite volume extrapolation for the mass of the  $\eta$ -meson at  $\beta = 12$  and different values of the hopping parameter  $\kappa$  compared to the smallest lattice momentum  $\pi/L_t$ . The horizontal lines indicate the infinite volume mass  $m$ .

the smallest value  $\kappa = 0.26206$  the infinite volume mass is given by  $m = 0.1607(8)$ . For our smallest lattice with  $L_t = 16$  it is below the smallest lattice momentum  $\pi/16$  and in accordance with the sampling theory we observe a more massive state then. For our largest lattices with  $L_t = 64$  and  $L_t = 96$  the mass  $m_L$  is within statistical errors the same as the infinite volume mass  $m$ . Qualitatively the same behaviour is observed for  $\kappa = 0.26344$  and  $\kappa = 0.26455$ . For  $\kappa = 0.26539$  all masses except the one on the largest lattice are below the lattice cutoff. Nevertheless we observe that the fit function works well even in this case and yields reliable results for the infinite volume mass. For the spectroscopy we restrict ourselves to a lattice size of  $64 \times 32$  and  $\kappa \leq 0.264$ , where finite volume effects are negligible.

## 5.2 Mesons

We have calculated the  $\pi$ -,  $\eta$ - and  $f$ -meson correlation function for different values of the hopping parameter  $\kappa$ . In Figure 8 we show our results for two different values of  $\kappa \leq \kappa_c$ . For the larger value  $\kappa = 0.26096$  the masses are slightly above the lattice momentum cutoff. First of all we observe that the  $\pi$ - and the  $\eta$ -meson correlation functions are not distinguishable for all values of  $\kappa$  considered. We conclude that the ground state mass of

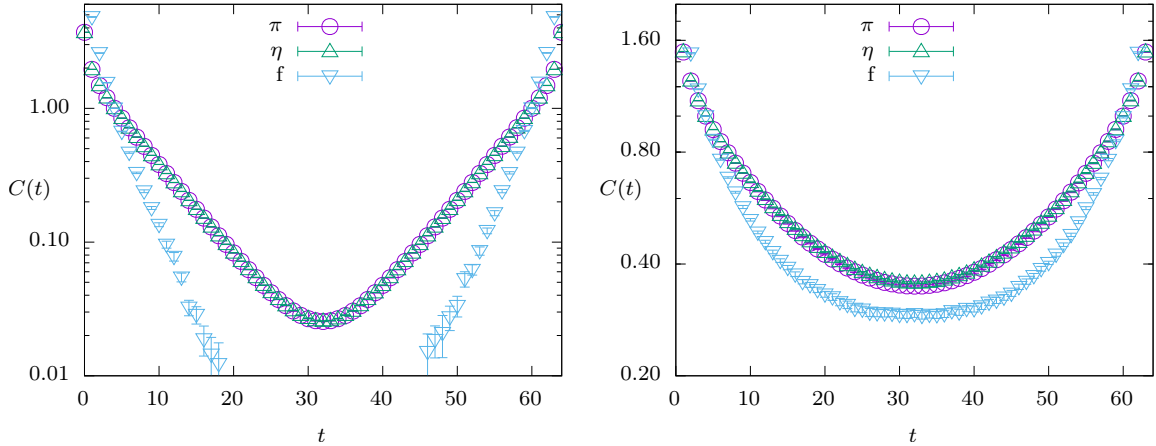


**Figure 8:** The  $\eta$ -,  $\pi$ - and  $f$ -meson correlation functions are shown for  $\beta = 17$  and  $\kappa = 0.25800$  (left) and  $\kappa = 0.26096$  (right).

the  $\eta$ -meson vanishes in the chiral limit. Next we observe that the correlation functions for the  $f$ - and the  $\eta$ -meson become more and more degenerate in the chiral limit. This suggests, that indeed both mesons form a multiplet in the chiral limit, independent of the restoration of susy in the continuum limit. To further investigate this behaviour we study the connected and the disconnected contributions to the correlation functions. Recall, that the pion correlation function is defined as the connected part of the  $\eta$ -meson correlation function. In Figure 9 we depicted the two contributions to the correlation functions for the  $\eta$ -meson (left) and the  $f$ -meson (right). For the  $\eta$ -meson we find that the connected part is

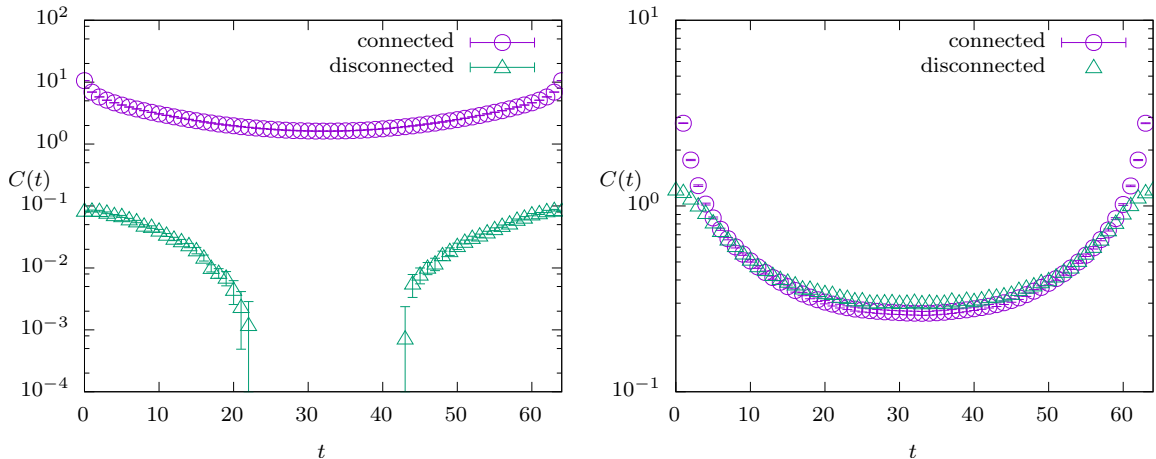


**Figure 9:** Connected and disconnected part of the  $\eta$ -meson (left) and  $f$ -meson (right) correlation function for  $\beta = 17$  and  $\kappa = 0.26096$ .

at least two orders of magnitude larger than the disconnected part. Therefore the  $\eta$ - and the  $\pi$ -meson correlation function are not distinguishable. For the  $f$ -meson we see, that both contributions are roughly of equal size over the whole  $t$  range. Hence a degeneracy between  $\eta$ -meson and  $f$ -meson correlation functions is nontrivial. We also determined the ground state and excited state masses of both mesons. The results are given in Table 8 as well as

in Figure 10. Again we observe that the masses for the  $\eta$  and  $\pi$  meson are the same for

$\beta = 14.0$							
$\kappa$	0.25800	0.26042	0.26178	0.26209	0.26240	0.26270	0.26302
$m_\eta$	0.208(1)	0.150(2)	0.107(1)	0.098(2)	0.082(3)	0.068(4)	0.053(1)
$m_f$	0.444(71)	0.322(12)	0.237(10)	0.195(11)	0.133(92)	0.084(45)	0.047(3)
$m_{\eta^*}$	0.889(21)	0.943(17)	0.358(54)	0.281(77)	0.272(97)	0.233(33)	0.218(32)
$m_{f^*}$	-	-	-	0.792(472)	0.313(246)	0.332(328)	0.242(7)
$\beta = 15.5$							
$\kappa$	0.25694	0.25907	0.26082	0.26113	0.26144	0.26175	0.26205
$m_\eta$	0.203(3)	0.154(1)	0.100(5)	0.089(2)	0.076(9)	0.059(2)	0.045(1)
$m_f$	0.479(37)	0.324(43)	0.197(11)	0.155(42)	0.100(29)	0.047(14)	0.035(3)
$m_{\eta^*}$	0.842(232)	0.927(11)	0.311(48)	0.270(39)	0.245(43)	0.216(33)	0.222(10)
$m_{f^*}$	-	-	-	0.380(415)	0.291(124)	0.253(89)	0.226(72)
$\beta = 17.0$							
$\kappa$	0.25562	0.25800	0.25961	0.25994	0.26028	0.26062	0.26096
$m_\eta$	0.208(3)	0.157(1)	0.112(2)	0.096(1)	0.082(1)	0.068(2)	0.053(3)
$m_f$	0.502(8)	0.336(26)	0.239(32)	0.159(31)	0.085(13)	0.061(1)	0.044(3)
$m_{\eta^*}$	-	0.951(14)	0.462(19)	0.0353(20)	0.283(62)	0.264(96)	0.213(15)
$m_{f^*}$	-	-	0.533(262)	0.509(216)	0.321(36)	0.302(24)	0.270(13)

**Table 8:** Masses of the  $\eta$ - and f-meson ground and excited states.

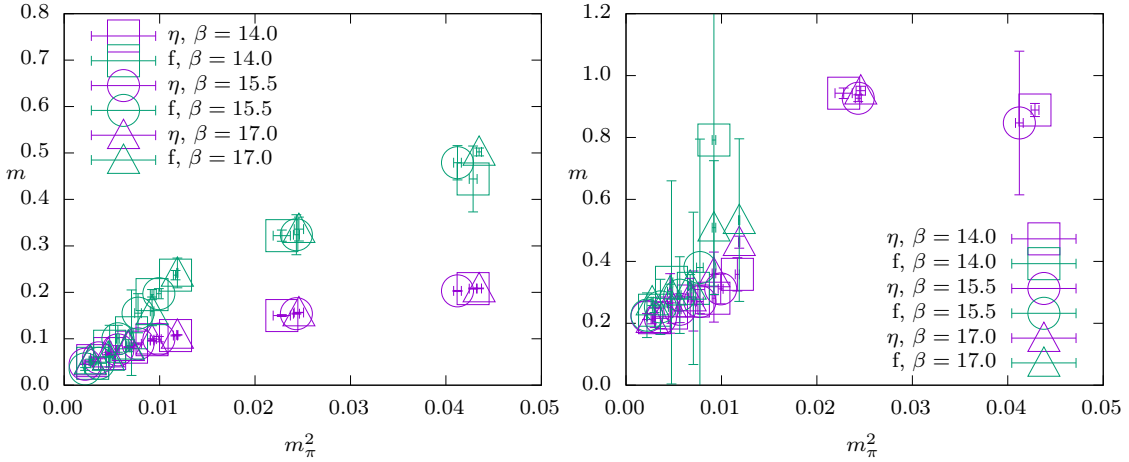


**Figure 10:** Ground (left) and excited (right) state masses of the  $\eta$ - and f-meson as function of the pion mass squared for  $\beta = 14, 15.5$  and 17.

all values of  $\beta$  and  $\kappa$ . For the ground state mass of the f-meson, we find agreement with the ground state mass of the  $\eta$ -meson only in the chiral limit.

For the excited states we can not make similar conclusive statements, since it is difficult to extract their masses from  $\kappa$ 's not close to  $\kappa_c$ . This explains the large errors for the masses

of the excited states. Nevertheless, in the chiral limit we find they are all in the same range spanning from 0.19 to 0.28. Since we were unable to get a better mass-resolution for these states, we can not make a reliable continuum extrapolation to arrive at physical masses. But we may safely conclude that in the chiral limit the  $\eta$ - and f-meson are degenerate. This remains true for all values of the gauge coupling considered such that this mass degeneracy still holds in the continuum limit. In addition, the ground state multiplet is massless, since the  $\eta$ -meson and the pion always have the same mass. Whether both mesons form the proposed super-multiplet depends on the mass of the gluino-gluonball.

### 5.3 Gluino-gluonball

In the four-dimensional multiplet we have two gluino-gluonball particles, which differ by their transformation under parity. The interpolating fermionic operator we use is given by

$$O_{GG} = \Sigma_{\mu\nu} F^{\mu\nu} \lambda. \quad (5.2)$$

Although the projectors on a definite parity quantum number are  $P_{\pm} = (1 \pm \Gamma_0)/2$  we project on periodic (S) and antiperiodic (A) correlation functions

$$C_A(t) = \langle O_{GG}(t) O_{GG}^\dagger(0) \rangle, \quad C_S(t) = \langle O_{GG}(t) \Gamma_0 O_{GG}^\dagger(0) \rangle. \quad (5.3)$$

All other contractions over  $\Gamma$ -matrices can be written as a linear combination of these two correlation functions, as expected for two independent physical states. The determina-

$S$	0	6	12	18	24	30	36
$m_A$	0.324(13)	0.531(29)	0.404(16)	0.358(13)	0.333(11)	0.315(10)	0.302(10)
$m_S$	0.391(12)	0.633(14)	0.517(7)	0.469(5)	0.441(4)	0.421(4)	0.406(4)
$S$	48	80	240	400	1200	2400	3600
$m_A$	0.282(9)	0.256(12)	0.234(5)	0.222(1)	0.165(2)	0.163(2)	0.168(2)
$m_S$	0.384(3)	0.347(11)	0.270(3)	0.252(2)	0.224(5)	0.214(4)	0.214(5)

**Table 9:** Extracted masses for different smearing levels  $S$  for the symmetric and antisymmetric gluino-gluonball states for  $\beta = 17$  and  $m_f = -0.084$ .

tion of the mass on larger lattices is only possible with the help of gauge field smearing. We introduce the smearing level  $S = \text{steps} \times \text{parameter}$ , where 'steps' are the amount of smearing steps and 'parameter' is the smearing parameter for these steps. The correlation functions  $C_S(t)$  for different smearing levels are shown in Figure 11 (left panel). Even for a large amount of smearing steps the signal still improves. In Table 9 we give our results for  $\beta = 17$  and  $m_f = -0.084$ . At first, smearing increases the mass of the state. This can be attributed to a contact interaction between almost decoupled gluonballs (see next chapter). For even more smearing levels, the mass decreases until it converges. This behaviour is even seen for large smearing levels ( $S = 3600$ ). Both masses  $m_A$  and  $m_S$  converge to the same value as expected in a parity symmetric theory. Furthermore the mass depends only

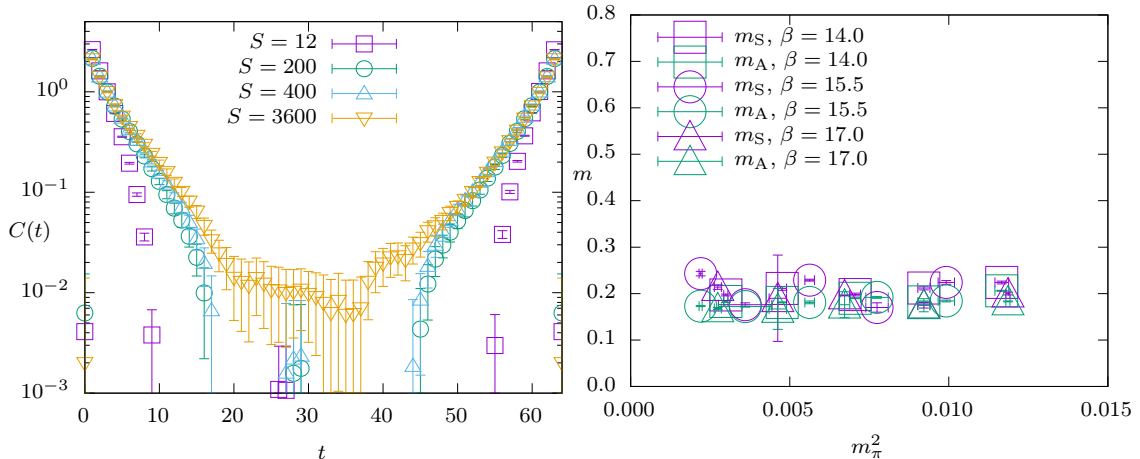


**Figure 11:** Left: Guino-gluon correlation function at  $\beta = 17$  and  $m_f = -0.084$  for different smearing levels  $S$ . Right: Guino-gluon mass as a function of the squared pion mass.

very weakly on the gauge coupling  $\beta$  and the bare fermion mass  $m_f$  (see Figure 11, right panel), but it depends on the lattice size. For the smearing level of 400, it decreases from  $m_s = 0.315(25)$  on the  $16 \times 8$  lattice to  $0.262(37)$  on the  $32 \times 16$  lattice and further to  $0.252(2)$  on our largest  $64 \times 32$  lattice. With (5.1) we can extrapolate to infinite volume. The limiting value 0.251 is very close to the value on the largest lattice, such that there are only small finite volume effects on the large lattice.

Comparing with the masses of the mesons, we find that the guino-gluoballs have comparable masses as the excited mesons. An explanation for this unexpected behavior could be, that the first excited state of the guino-gluoball dominates the correlation function over a long  $t$ -range, such that the ground state contribution is not visible on our lattice sizes. To see whether this is the case, we applied this large amount of smearing ( $S = 3600$ ), but we did not observe any sign of a lighter particle in this channel. Thus an alternative explanation could be, that we indeed detected the ground state of the guino-gluoball. But then one must explain why the guino-gluoball forms a multiplet with the excited mesons and not the mesons in their ground states. The fermionic state in the VY-multiplet is a mixture of the guino-gluon and a guino-scalarball. Possibly the guino-scalarball has a lighter mass. Unfortunately, also with a large amount of smearing for the scalar field, we are not able to obtain an estimate for its mass.

#### 5.4 Glue- and scalarballs

The second multiplet of bound states consists of glue-, scalar- and glue-scalarballs. The correlation functions of the corresponding interpolating operators show no correlation at all for large distances. For the glueball, this is shown in Figure 12. The only nonzero values of the correlation function are at distances  $t = 0, 1, 62$  and  $64$ . A similar behavior is seen in pure Yang-Mills theory on a two-dimensional lattice. Indeed, with Migdals prescription [72] one obtains for the correlation function of the glueball operator  $G(x)$  in this theory

$$\langle G(x)G^\dagger(y) \rangle = C_G = \text{const.} \quad (5.4)$$

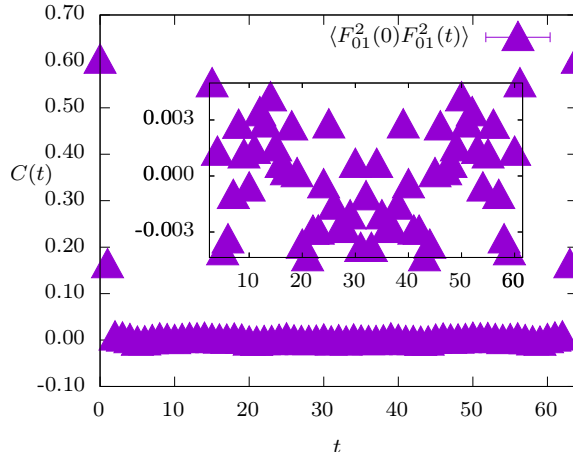


**Figure 12:** Glueball Correlation function for  $\beta = 17$  and  $m_f = -0.074$ .

This holds true if the supports of the interpolating operators are disjoint. Hence the correlation function of glueballs will show only a correlation between time slices with distance less than the diameter  $A_G$  of the support of  $G(x)$ . We observe the very same behaviour in the supersymmetric theory in Figure 12, where the diameter is two. In the continuum limit, the physical diameter shrinks to zero and the expectation value is constant in the whole spacetime volume. Furthermore one can show, that this value goes to zero and the glueball decouples from the theory. This lattice result is in agreement with the analytical result presented in [73].

Since we use smearing of sources and sinks in our analysis, it maybe instructive to study the effect of smearing on the correlation function of glueballs. Every smearing step increases the diameter  $A_G$ , and thus induces more artificial correlations between the lattice points, which are uncorrelated without smearing. The results can be seen in Figure 13, where we compare pure Yang-Mills theory (left) to susy Yang-Mills theory (right). In both cases we observe more nonzero values in the correlation functions for higher smearing levels, as expected. Smearing effects can also be seen in the effective mass: in both theories it is an ever increasing function of the distance for all values of the smearing level. We conclude that, similarly as in pure YM-theory in two dimensions, there is no correlation for glueballs which means that the glueball completely decouples from the  $\mathcal{N} = (2, 2)$  SYM-theory in two dimensions. Similarly we did observe no correlations for the scalarball and glue-scalarball. Since they should form a super-multiplet with the glueball, they will decouple from the theory as well. The additional gluino-glueball state present in the super-multiplet will also show no correlations, and thus is not seen in our simulations.

## 6 Conclusions

In our work, we simulated the two-dimensional  $\mathcal{N} = (2, 2)$  SYM lattice-theory in a conventional approach without twisting. The simulation could be afflicted with two potentially serious problems common in gauge theories with extended supersymmetry: flat directions and a sign problem. In the present work we demonstrate that these problems do not arise

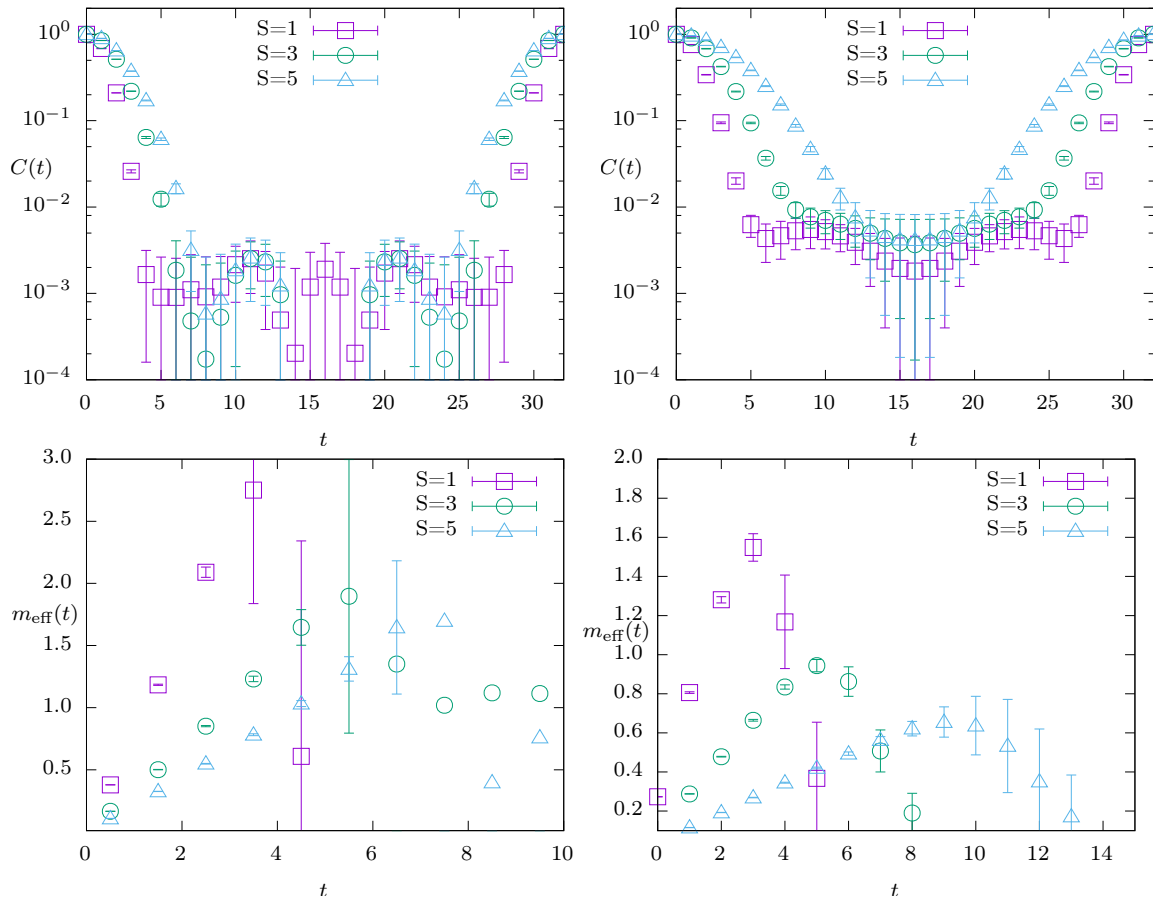


**Figure 13:** Comparison between the Glueball correlation function for the two dimensional Yang-Mills theory (left) and the two-dimensional Super Yang-Mills theory (right) for different smearing levels  $S$ . In the bottom row we plot the effective mass.

for all parameters which are relevant to approach the supersymmetric continuum limit. As concerning the sign problem, this is related to the absence of the sign problem in the  $\mathcal{Q}$ -exact formulation of the continuum theory [74].

When studying various Ward identities, we did observe that they are rather insensitive to the bare mass of the scalars  $m_s$ , as long as the latter is in the vicinity of the (all-loop) perturbative value in the supersymmetric continuum model, which is given by  $m_s^2 = 0.65948255(8)$ . In our simulations we used a mass close to this values. Away from the continuum limit this may not be the optimal choice. Spotting an observable, which allows for further fine-tuning of the scalar mass on the lattice could perhaps improve the results and would allow for more accurate predictions. But such an improvement is probably not easy to achieve since our results are stable and reliable. They do not depend on the scalar mass in the vicinity of the above value and thus a further fine-tuning of  $m_s$  does not help much.

The restoration of supersymmetry is observed in the chiral limit. Since the fermion mass is not a relevant coupling (contrary to the situation in four dimensions) this may come

as a surprise. But generally speaking fine-tuning of an irrelevant coupling maybe helpful away from criticality. In any case, the result confirms the assumption, that supersymmetry is recovered in the chiral limit, similarly as in the four-dimensional mother-theory. But the spectrum of bound states looks different than in the four-dimensional  $\mathcal{N} = 1$  theory. We found a massless multiplet – the dimensionally reduced Veneziano-Yankielowicz multiplet – which contains the mesons, while the Farrar-Gabadadze-Schwetz multiplet decouples from the theory (see Table 10). The mass of the lightest gluino-glueball seen in the simulations

particle	$m$	$m^*$
a- $\eta$	0.053(3) $\rightarrow$ 0	0.213(15)
f	0.044(3) $\rightarrow$ 0	0.270(13)
gluino-glueball	–	0.168(2)/0.214(5)

**Table 10:** We observe the formation of a massive VY-multiplet while the ground states are massless. The FGS-multiplet decouples from the theory.

is still a bit ambiguous. Within errors its mass is equal to that of the excited mesons. We believe we could not follow the corresponding correlation function for large enough  $t$ -values, in order to disentangle the signals from the ground state and excited state. Probably we did only see the excited gluino-glueball which forms a multiplet with the excited meson states. If this is true, then finding the missing ground state of the gluino-glueball maybe as difficult as finding a needle in a haystack.

In future studies we intend to study the phase structure of the  $\mathcal{N} = (2, 2)$  SYM-theory as well as related systems with more supersymmetries. It would be interesting to measure the two independent holonomies (Wilson loops with windings) on the two-torus and their dependence on the geometry of the torus. This way one could first compare with results obtained with  $\mathcal{Q}$ -exact formulations for  $\mathcal{N} = (8, 8)$  SYM-theory [75] and furthermore extend to systems with less supersymmetry where no  $\mathcal{Q}$ -exact formulation exists. Since we did not encounter any sign problems for  $\kappa < \kappa_c$  and since the flat directions are stabilized, we should be able to accurately localize the expected phases and phase-transition lines in two-dimensional SYM with extended supersymmetry.

## Acknowledgments

We thank Georg Bergner, Marc Steinhauser and Masanori Hanada for fruitful discussions and comments. D.A. and B.W. were supported by the DFG Research Training Group 1523/2 “Quantum and Gravitational Fields” and in part by the DFG (Grant Wi 777/11). The simulations were performed at the HPC-Cluster OMEGA of the University Jena.

## A Exact lattice Ward identities

In the main body of the text we studied the violation of several Ward identities due to lattice artifacts. Thereby we neglected contributions stemming from  $m_f$  and  $m_s$  deviating

from their critical values. Here we derive lattice Ward identities without any approximation. The application of the lattice supersymmetry transformations (4.1) to the lattice Lagrangian results in

$$\begin{aligned}\bar{Q}^\alpha \mathcal{L}_{\text{lat}} &= \frac{\beta}{2} \left\{ \partial_\mu s_\mu^\alpha - 2m_f (\Gamma_{MN})^{\alpha\beta} F^{MN} \lambda_\beta + 2m_s^2 (\Gamma_{m+1})^\alpha{}_\beta \lambda^\beta \phi^m \right\} + X_S \\ &= \frac{\beta}{2} \left\{ \partial_\mu s_\mu^\alpha - m_f \chi_f^\alpha + m_s^2 \chi_s^\alpha \right\} + X_S,\end{aligned}\tag{A.1}$$

with

$$\chi_f^\alpha = 2 \text{tr} (\Gamma_{MN}^{\alpha\beta} F^{MN} \lambda_\beta) \quad \text{and} \quad \chi_s^\alpha = 2 \text{tr} (\Gamma_{m+1}^{\alpha\beta} \lambda_\beta \phi^m).\tag{A.2}$$

The contributions  $\chi^\alpha$  originate from the fermion and scalar mass terms introduced in the lattice Lagrangian. As pointed out previously the supercurrent  $s_\mu^\alpha$  vanishes after summation over the lattice sites. The term  $X_S$  originates from the lattice regularisation and is of order  $\mathcal{O}(a)$ . Clearly, at tree-level supersymmetry is restored in the continuum limit for the critical values  $m_f^c = m_s^c = 0$ . At one-loop a finite scalar mass is generated due to different lattice momenta of bosons and fermions. Furthermore, the Wilson term in the fermion operator gives rise to a nonzero critical fermion mass. In the continuum limit, no further corrections are generated at higher loop order such that  $m_f^c \rightarrow 0$ . In order to compensate for the shifts at finite lattice spacing one adds counter-terms to the tree-level lattice action and ends up with the full quantum lattice Ward identity (4.3). The scalar mass counter-term must also be included in the Ward identity  $W_3$  and the bosonic Ward identity because they contain the kinetic term for the scalar fields. Thus, the set of lattice Ward identities read

$$\begin{aligned}W_B &= \beta V^{-1} \langle S_B \rangle + \beta m_s^2 \langle \text{tr} \phi^2 \rangle + \beta \langle \text{tr} \bar{\lambda} \Gamma^{MN} F_{MN} \Theta \rangle \rightarrow \frac{9}{2}, \\ W_3 &= \frac{\beta}{2} \langle \text{tr} D_\mu \phi^a D^\mu \phi_a \rangle + \beta m_s^2 \langle \text{tr} \phi^2 \rangle + 2\beta \langle \text{tr} \bar{\lambda} \Gamma^{\mu m} D_\mu \phi_m \Theta \rangle \rightarrow 3, \\ W_2 &= \frac{\beta}{4} \langle \text{tr} F_{\mu\nu} F^{\mu\nu} \rangle + \beta \langle \text{tr} \bar{\lambda} \Upsilon \rangle + \beta \langle \text{tr} \bar{\lambda} \Gamma^{\mu\nu} F_{\mu\nu} \Theta \rangle \rightarrow \frac{3}{2}, \\ W_1 &= \frac{\beta}{2} \langle \text{tr} [\phi_1, \phi_2]^2 \rangle - \beta \langle \text{tr} \bar{\lambda} \Upsilon \rangle + \beta \langle \text{tr} \bar{\lambda} \Gamma^{mn} [\phi_m, \phi_n] \Theta \rangle \rightarrow 0,\end{aligned}\tag{A.3}$$

where we used the abbreviations

$$\Theta = \left( m_s^2 - (m_s^c)^2 \right) \chi_s - (m_f - m_f^c) \chi_f, \quad \Upsilon = \frac{i}{8} (\Gamma_2 [\phi_1, \lambda] + \Gamma_3 [\phi_2, \lambda]).\tag{A.4}$$

Near the supersymmetric continuum limit, lattice artifacts should be sufficiently suppressed such that the breaking of Ward identities originate from the missing fine-tuning of  $m_f^c$  and  $m_s^c$ . Since we anyway use the  $\pi$ -mass to fine-tune  $m_f^c$  we will focus on the fine-tuning of  $m_s^c$  in what follows. We will show this fine-tuning approach for the Ward-identity  $W_2$ . The results for the other identities are very similar.

First we introduce  $W_2^b$  and the correction terms  $\mathcal{C}_s$  and  $\mathcal{C}_f$

$$W_2^b = \beta \left\langle \frac{1}{4} \text{tr} F_{\mu\nu} F^{\mu\nu} + \text{tr} \bar{\lambda} \Upsilon \right\rangle, \quad \mathcal{C}_s = \beta \langle \text{tr} \bar{\lambda} \Gamma^{\mu\nu} F_{\mu\nu} \chi_s \rangle, \quad \mathcal{C}_f = \beta \langle \text{tr} \bar{\lambda} \Gamma^{\mu\nu} F_{\mu\nu} \chi_f \rangle,\tag{A.5}$$

which enter the Ward identity  $W_2$  of interest,

$$W_2 = W_2^b + (m_s^2 - (m_s^c)^2) \mathcal{C}_s + (m_f - m_f^c) \mathcal{C}_f. \quad (\text{A.6})$$

Now we simulate the gauge theory for a set of values  $m_s^2$  near the one-loop value 0.65948 and measure the expectation values  $W_2^b$ ,  $\mathcal{C}_s$  and  $\mathcal{C}_f$ . Note that  $m_s$  and  $m_f$  are the masses used to generate the ensemble, whereas the trial mass  $m_s^c$  only enters via the operators defining the Ward identities. Next we should extract a trial mass for which  $W_2 \approx \frac{3}{2}$  for all  $m_s$  near the critical value. Note that the extracted  $m_s^c$  could deviate from the one-loop results due to lattice artifacts.

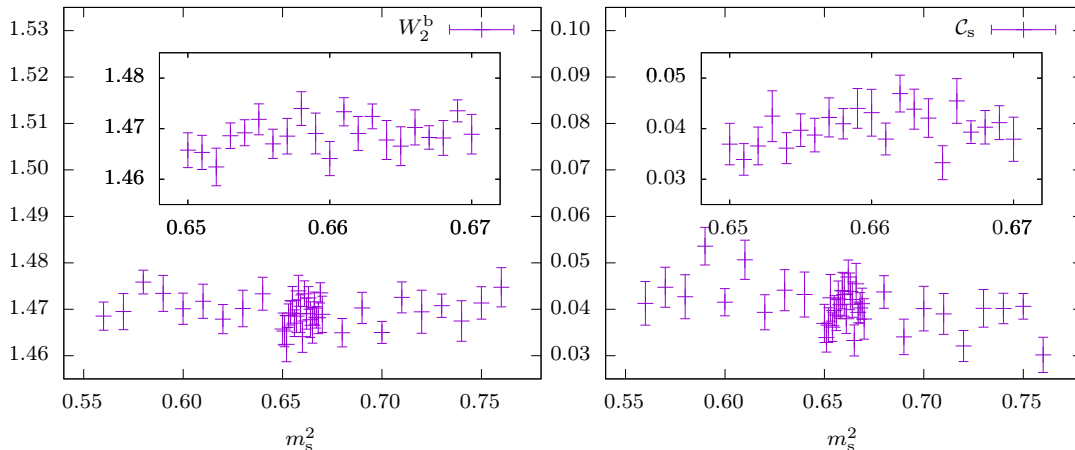


**Figure 14:** On the left we see the term  $W_2^b$  and on the right the term  $\mathcal{C}_s$ . The inserts show the values near the critical value of  $m_s^2$ .

Figure 14 clearly shows that  $W_2^b$  and  $\mathcal{C}_s$  do not depend sensitively on  $m_s$  near the critical one-loop value. The same holds true for  $\mathcal{C}_f$ , which is not shown in the figure. This means that it is difficult to find any deviations of  $m_s^c$  from its known continuum one-loop value. But since the correction terms  $\mathcal{C}_s$  and  $\mathcal{C}_f$  in (A.6) are two orders of magnitude smaller than  $W_2^b$  we may safely neglect the lattice correction  $\Theta$  if we are close to the critical masses, which we ensure by extrapolating to the chiral limit and using  $m_s = 0.66$ . This leads to the final set of approximate Ward identities (4.4) which are measured in our simulations.

## References

- [1] A. Salam and J. A. Strathdee, *Supersymmetry and Nonabelian Gauges*, *Phys. Lett.* **51B** (1974) 353–355.
- [2] S. Ferrara and B. Zumino, *Supergauge Invariant Yang-Mills Theories*, *Nucl. Phys.* **B79** (1974) 413.
- [3] D. Amati, K. Konishi, Y. Meurice, G. C. Rossi and G. Veneziano, *Nonperturbative Aspects in Supersymmetric Gauge Theories*, *Phys. Rept.* **162** (1988) 169–248.
- [4] G. Veneziano and S. Yankielowicz, *An Effective Lagrangian for the Pure  $N=1$  Supersymmetric Yang-Mills Theory*, *Phys. Lett.* **113B** (1982) 231.

- [5] G. R. Farrar, G. Gabadadze and M. Schwetz, *The spectrum of softly broken  $N=1$  supersymmetric Yang-Mills theory*, *Phys. Rev.* **D60** (1999) 035002, [[hep-th/9806204](#)].
- [6] G. R. Farrar, G. Gabadadze and M. Schwetz, *On the effective action of  $N=1$  supersymmetric Yang-Mills theory*, *Phys. Rev.* **D58** (1998) 015009, [[hep-th/9711166](#)].
- [7] A. Feo, P. Merlatti and F. Sannino, *Information on the super Yang-Mills spectrum*, *Phys. Rev.* **D70** (2004) 096004, [[hep-th/0408214](#)].
- [8] G. Curci and G. Veneziano, *Supersymmetry and the Lattice: A Reconciliation?*, *Nucl. Phys.* **B292** (1987) 555–572.
- [9] J. Giedt, R. Brower, S. Catterall, G. T. Fleming and P. Vranas, *Lattice super-Yang-Mills using domain wall fermions in the chiral limit*, *Phys. Rev.* **D79** (2009) 025015, [[0810.5746](#)].
- [10] M. G. Endres, *Dynamical simulation of  $N=1$  supersymmetric Yang-Mills theory with domain wall fermions*, *Phys. Rev.* **D79** (2009) 094503, [[0902.4267](#)].
- [11] JLQCD collaboration, S. W. Kim, H. Fukaya, S. Hashimoto, H. Matsufuru, J. Nishimura and T. Onogi, *Lattice study of 4d  $N=1$  super Yang-Mills theory with dynamical overlap gluino*, *PoS LATTICE2011* (2011) 069, [[1111.2180](#)].
- [12] I. Montvay, *SUSY on the lattice*, *Nucl. Phys. Proc. Suppl.* **63** (1998) 108–113, [[hep-lat/9709080](#)].
- [13] DESY-MUNSTER collaboration, I. Campos, R. Kirchner, I. Montvay, J. Westphalen, A. Feo, S. Luckmann et al., *Monte Carlo simulation of  $SU(2)$  Yang-Mills theory with light gluinos*, *Eur. Phys. J.* **C11** (1999) 507–527, [[hep-lat/9903014](#)].
- [14] DESY-MUNSTER-ROMA collaboration, F. Farchioni, C. Gebert, R. Kirchner, I. Montvay, A. Feo, G. Munster et al., *The Supersymmetric Ward identities on the lattice*, *Eur. Phys. J.* **C23** (2002) 719–734, [[hep-lat/0111008](#)].
- [15] I. Montvay, *Supersymmetric Yang-Mills theory on the lattice*, *Int. J. Mod. Phys.* **A17** (2002) 2377–2412, [[hep-lat/0112007](#)].
- [16] G. Münster and H. Stüwe, *The mass of the adjoint pion in  $\mathcal{N} = 1$  supersymmetric Yang-Mills theory*, *JHEP* **05** (2014) 034, [[1402.6616](#)].
- [17] G. Bergner, P. Giudice, G. Münster, S. Piemonte and D. Sandbrink, *Phase structure of the  $\mathcal{N} = 1$  supersymmetric Yang-Mills theory at finite temperature*, *JHEP* **11** (2014) 049, [[1405.3180](#)].
- [18] G. Bergner and S. Piemonte, *Compactified  $\mathcal{N} = 1$  supersymmetric Yang-Mills theory on the lattice: continuity and the disappearance of the deconfinement transition*, *JHEP* **12** (2014) 133, [[1410.3668](#)].
- [19] G. Bergner, P. Giudice, G. Münster, I. Montvay and S. Piemonte, *The light bound states of supersymmetric  $SU(2)$  Yang-Mills theory*, *JHEP* **03** (2016) 080, [[1512.07014](#)].
- [20] S. Ali, G. Bergner, H. Gerber, P. Giudice, G. Münster, I. Montvay et al., *The light bound states of  $\mathcal{N} = 1$  supersymmetric  $SU(3)$  Yang-Mills theory on the lattice*, [1801.08062](#).
- [21] M. Steinhauser, A. Sternbeck, B. Wellegehausen and A. Wipf, *Spectroscopy of four-dimensional  $\mathcal{N} = 1$  supersymmetric  $SU(3)$  Yang-Mills theory*, in *35th International Symposium on Lattice Field Theory (Lattice 2017) Granada, Spain, June 18-24, 2017*, 2017, [1711.05086](#), <http://inspirehep.net/record/1636206/files/arXiv:1711.05086.pdf>.

- [22] H. Suzuki and Y. Taniguchi, *Two-dimensional  $N = (2,2)$  super Yang-Mills theory on the lattice via dimensional reduction*, *JHEP* **10** (2005) 082, [[hep-lat/0507019](#)].
- [23] H. Fukaya, I. Kanamori, H. Suzuki and T. Takimi, *Numerical results of two-dimensional  $N=(2,2)$  super Yang-Mills theory*, *PoS LAT2007* (2007) 264, [[0709.4076](#)].
- [24] E. Witten, *Bound states of strings and p-branes*, *Nucl. Phys.* **B460** (1996) 335–350, [[hep-th/9510135](#)].
- [25] H. Fukaya, I. Kanamori, H. Suzuki, M. Hayakawa and T. Takimi, *Note on massless bosonic states in two-dimensional field theories*, *Prog. Theor. Phys.* **116** (2007) 1117–1129, [[hep-th/0609049](#)].
- [26] F. Antonuccio, H. C. Pauli, S. Pinsky and S. Tsujimaru, *DLCQ bound states of  $N=(2,2)$  superYang-Mills at finite and large  $N$* , *Phys. Rev.* **D58** (1998) 125006, [[hep-th/9808120](#)].
- [27] M. Harada, J. R. Hiller, S. Pinsky and N. Salwen, *Improved results for  $N=(2,2)$  super Yang-Mills theory using supersymmetric discrete light-cone quantization*, *Phys. Rev.* **D70** (2004) 045015, [[hep-th/0404123](#)].
- [28] K. Hori and D. Tong, *Aspects of Non-Abelian Gauge Dynamics in Two-Dimensional  $N=(2,2)$  Theories*, *JHEP* **05** (2007) 079, [[hep-th/0609032](#)].
- [29] S. Catterall, R. G. Jha and A. Joseph, *Nonperturbative study of dynamical SUSY breaking in  $\mathcal{N} = (2, 2)$  Yang-Mills*, [1801.00012](#).
- [30] A. G. Cohen, D. B. Kaplan, E. Katz and M. Unsal, *Supersymmetry on a Euclidean space-time lattice. 2. Target theories with eight supercharges*, *JHEP* **12** (2003) 031, [[hep-lat/0307012](#)].
- [31] S. Catterall, *A Geometrical approach to  $N=2$  super Yang-Mills theory on the two dimensional lattice*, *JHEP* **11** (2004) 006, [[hep-lat/0410052](#)].
- [32] F. Sugino, *A Lattice formulation of superYang-Mills theories with exact supersymmetry*, *JHEP* **01** (2004) 015, [[hep-lat/0311021](#)].
- [33] S. Matsuura and F. Sugino, *Lattice formulation for  $2d = (2, 2), (4, 4)$  super Yang-Mills theories without admissibility conditions*, *JHEP* **04** (2014) 088, [[1402.0952](#)].
- [34] S. Catterall, *Simulations of  $N=2$  super Yang-Mills theory in two dimensions*, *JHEP* **03** (2006) 032, [[hep-lat/0602004](#)].
- [35] S. Catterall, *First results from simulations of supersymmetric lattices*, *JHEP* **01** (2009) 040, [[0811.1203](#)].
- [36] I. Kanamori and H. Suzuki, *Restoration of supersymmetry on the lattice: Two-dimensional  $N = (2,2)$  supersymmetric Yang-Mills theory*, *Nucl. Phys.* **B811** (2009) 420–437, [[0809.2856](#)].
- [37] H. Suzuki, *Two-dimensional  $N = (2,2)$  super Yang-Mills theory on computer*, *JHEP* **09** (2007) 052, [[0706.1392](#)].
- [38] I. Kanamori and H. Suzuki, *Some physics of the two-dimensional  $N = (2,2)$  supersymmetric Yang-Mills theory: Lattice Monte Carlo study*, *Phys. Lett.* **B672** (2009) 307–311, [[0811.2851](#)].
- [39] I. Kanamori, F. Sugino and H. Suzuki, *Observing dynamical supersymmetry breaking with euclidean lattice simulations*, *Prog. Theor. Phys.* **119** (2008) 797–827, [[0711.2132](#)].
- [40] D. Kadoh and H. Suzuki, *SUSY WT identity in a lattice formulation of  $2D = (2,2)$  SYM*, *Phys. Lett.* **B682** (2010) 466–471, [[0908.2274](#)].

- [41] T. Takimi, *Relationship between various supersymmetric lattice models*, *JHEP* **07** (2007) 010, [[0705.3831](#)].
- [42] P. H. Damgaard and S. Matsuura, *Lattice Supersymmetry: Equivalence between the Link Approach and Orbifolding*, *JHEP* **09** (2007) 097, [[0708.4129](#)].
- [43] P. H. Damgaard and S. Matsuura, *Relations among Supersymmetric Lattice Gauge Theories via Orbifolding*, *JHEP* **08** (2007) 087, [[0706.3007](#)].
- [44] M. Unsal, *Twisted supersymmetric gauge theories and orbifold lattices*, *JHEP* **10** (2006) 089, [[hep-th/0603046](#)].
- [45] D. B. Kaplan, *Recent developments in lattice supersymmetry*, *Nucl. Phys. Proc. Suppl.* **129** (2004) 109–120, [[hep-lat/0309099](#)].
- [46] J. Giedt, *Deconstruction and other approaches to supersymmetric lattice field theories*, *Int. J. Mod. Phys.* **A21** (2006) 3039–3094, [[hep-lat/0602007](#)].
- [47] S. Catterall, D. B. Kaplan and M. Unsal, *Exact lattice supersymmetry*, *Phys. Rept.* **484** (2009) 71–130, [[0903.4881](#)].
- [48] A. Joseph, *Supersymmetric Yang-Mills theories with exact supersymmetry on the lattice*, *Int. J. Mod. Phys.* **A26** (2011) 5057–5132, [[1110.5983](#)].
- [49] G. Bergner and S. Catterall, *Supersymmetry on the lattice*, *Int. J. Mod. Phys.* **A31** (2016) 1643005, [[1603.04478](#)].
- [50] S. Matsuura, T. Misumi and K. Ohta, *Topologically twisted  $N = (2, 2)$  supersymmetric Yang–Mills theory on an arbitrary discretized Riemann surface*, *PTEP* **2014** (2014) 123B01, [[1408.6998](#)].
- [51] S. Kamata, S. Matsuura, T. Misumi and K. Ohta, *Anomaly and sign problem in  $\mathcal{N} = (2, 2)$  SYM on polyhedra: Numerical analysis*, *PTEP* **2016** (2016) 123B01, [[1607.01260](#)].
- [52] S. Kamata, S. Matsuura, T. Misumi and K. Ohta, *Numerical Analysis of Discretized  $\mathcal{N} = (2, 2)$  SYM on Polyhedra*, *PoS LATTICE2016* (2016) 210, [[1612.01968](#)].
- [53] I. Montvay, *Majorana fermions on the lattice*, 2001, [[hep-lat/0108011](#)].
- [54] H. Nicolai, *A Possible constructive approach to (SUPER  $\phi^{**3}$ ) in four-dimensions. 1. Euclidean formulation of the model*, *Nucl. Phys.* **B140** (1978) 294–300.
- [55] P. van Nieuwenhuizen and A. Waldron, *On Euclidean spinors and Wick rotations*, *Phys. Lett.* **B389** (1996) 29–36, [[hep-th/9608174](#)].
- [56] M. Luscher and P. Weisz, *On-Shell Improved Lattice Gauge Theories*, *Commun. Math. Phys.* **97** (1985) 59.
- [57] A. D. Kennedy, I. Horvath and S. Sint, *A New exact method for dynamical fermion computations with nonlocal actions*, *Nucl. Phys. Proc. Suppl.* **73** (1999) 834–836, [[hep-lat/9809092](#)].
- [58] M. A. Clark and A. D. Kennedy, *The RHMC algorithm for two flavors of dynamical staggered fermions*, *Nucl. Phys. Proc. Suppl.* **129** (2004) 850–852, [[hep-lat/0309084](#)].
- [59] M. A. Clark, P. de Forcrand and A. D. Kennedy, *Algorithm shootout: R versus RHMC*, *PoS LAT2005* (2006) 115, [[hep-lat/0510004](#)].
- [60] M. A. Clark, *The Rational Hybrid Monte Carlo Algorithm*, *PoS LAT2006* (2006) 004, [[hep-lat/0610048](#)].

- [61] D. August, B. Wellegehausen and A. Wipf, *Spectroscopy of two dimensional  $N=2$  Super Yang Mills theory*, *PoS LATTICE2016* (2016) 234, [[1611.00551](#)].
- [62] A. Donini, M. Guagnelli, P. Hernandez and A. Vladikas, *Quenched spectroscopy for the  $N=1$  superYang-Mills theory*, *Nucl. Phys. Proc. Suppl.* **63** (1998) 718–720, [[hep-lat/9708006](#)].
- [63] R. Sommer, *A New way to set the energy scale in lattice gauge theories and its applications to the static force and alpha-s in  $SU(2)$  Yang-Mills theory*, *Nucl. Phys.* **B411** (1994) 839–854, [[hep-lat/9310022](#)].
- [64] C. Morningstar and M. J. Peardon, *Analytic smearing of  $SU(3)$  link variables in lattice QCD*, *Phys. Rev.* **D69** (2004) 054501, [[hep-lat/0311018](#)].
- [65] S. Gusken, U. Low, K. H. Mutter, R. Sommer, A. Patel and K. Schilling, *Nonsinglet Axial Vector Couplings of the Baryon Octet in Lattice QCD*, *Phys. Lett.* **B227** (1989) 266–269.
- [66] UKQCD collaboration, C. R. Allton et al., *Gauge invariant smearing and matrix correlators using Wilson fermions at  $\beta = 6.2$* , *Phys. Rev.* **D47** (1993) 5128–5137, [[hep-lat/9303009](#)].
- [67] Y. Taniguchi, *One loop calculation of SUSY Ward-Takahashi identity on lattice with Wilson fermion*, *Phys. Rev.* **D63** (2000) 014502, [[hep-lat/9906026](#)].
- [68] S. Luckmann, *Ward-Identitäten in der  $N=1$  Super-Yang-Mills-Theorie*, Diplomarbeit, University of Münster, 1997.
- [69] T. Galla, *Supersymmetrische und Chirale Ward-Identitäten in einer diskretisierten  $N=1$ -SUSY-Yang-Mills-Theorie*, Diplomarbeit, University of Münster, 1999.
- [70] G. Munster, *The Size of Finite Size Effects in Lattice Gauge Theories*, *Nucl. Phys.* **B249** (1985) 659–671.
- [71] M. Luscher, *Volume Dependence of the Energy Spectrum in Massive Quantum Field Theories. 1. Stable Particle States*, *Commun. Math. Phys.* **104** (1986) 177.
- [72] A. A. Migdal, *Recursion Equations in Gauge Theories*, *Sov. Phys. JETP* **42** (1975) 413.
- [73] N. E. Bralic, *Exact Computation of Loop Averages in Two-Dimensional Yang-Mills Theory*, *Phys. Rev.* **D22** (1980) 3090.
- [74] S. Catterall, R. Galvez, A. Joseph and D. Mehta, *On the sign problem in 2D lattice super Yang-Mills*, *JHEP* **01** (2012) 108, [[1112.3588](#)].
- [75] S. Catterall, R. G. Jha, D. Schaich and T. Wiseman, *Testing holography using lattice super-Yang-Mills on a 2-torus*, [1709.07025](#).